UNIVERSITÀ
DEGLI STUDI
DI PADOVA

Dipartimento di Ingegneria Industriale

LAUREA MAGISTRALE IN INGEGNERIA AEROSPAZIALE
LM-20

Experimental analysis of atmospheric plasma treatment and resin optimization for adhesive bonding of carbon fiber/epoxy composites

Relatore: Giovanni Lucchetta

Laureando:Julien Antonello

Matr. 1063591

A. A. 2014/2015

Contents

List of Figures

List of Tables

Abstract

In this investigation, two objectives have been pursued: the effects of atmospheric pressure plasma treatment on the surface of carbon fiber composites reinforced with phenolic resin matrix, with the goal of increase wettability and adhesion of epoxy resin, and the search of the best air bubble removal techniques for epoxy resin.

A substantial improvement in the surface wettability of carbon fiber composites is observed with drop contact angle measurements after the atmospheric plasma treatment. The plasma has been created using three different gas mix (He, He with 1% O2, He with 1% N2), than the best working gas has been found. Adding 1% of O2 or N2 to helium increases effectiveness of the plasma in polymer surface modification. It is observed that the surface modification of carbon fiber plate by atmospheric pressure plasma increases both surface energy and bonded joint strength. Scanning electron microscopy of untreated and atmospheric plasma treated specimens is carried out to examine the surface morphology. XPS and FTIR investigations have been conducted to find out the chemical composition and modifications of the surface. The improvement in adhesion properties of these materials is correlated with lap shear strength of adhesive bonded joints. Lap shear tests results for these materials show 40% improvement in joint strength after atmospheric plasma treatment.

The air bubble removal from the epoxy resin is studied using various method. It is observed that the more efficient method is done combining vacuum degassing with heating the substrate. This allows

a more dense epoxy with less failure risks due to air presence.

1 Introduction

In recent times, considerable efforts are being made for the development of new composite and polymeric materials with higher strength to weight ratio as well as thermomechanical properties. These materials are often used by adhesive bonding to form structural components. The adhesive bonding technique has shown itself capable of replacing conventional joining methods such as riveting, welding, and mechanical fastening in a variety of applications because of better fatigue performance and high strength to weight ratio [1,2].

Stress concentration is caused by mechanical methods and the overall load capacity of the structure is reduced [3]. An adhesive joint can distribute the applied load over the entire bonded area with more uniform stress distribution [3,4].

The use of adhesive bonding for aerospace application was restricted due to low thermal and mechanical properties of adhesives. However, due to the development of high performance adhesives, the use of bonding technique in space industry has been increased rapidly in last few decades. In this context, recently developed epoxy resins have excellent resistance to most acids, alkalis, solvents, corrosive agents, radiation [5], making it extremely interesting and useful for aeronautic and space applications.

The application of this research is about new generation drones with wings connected to the body by using an adhesive bonding.

Polymers have excellent bulk physical and chemical properties, are cheap, and easy to treat. However, very often they do not possess the surface prop-

erties needed for better adhesive bonding. They are normally hydrophobic and in general show insufficient adhesive bond strength due to relatively low surface energy [6]. For successful application of polymers to form structural parts using adhesive bonding (particular and important interest of aerospace industry), they need to have special surface properties like hydrophilicity [7] and correct chemical groups. Due to these reasons, surface preparation of polymeric adherends is then most important factor in the adhesive bonding process.

The main purpose of surface preparation is to improve the adhesion properties to such an extent that adhesive failure does not take place. This research focuses on carbon fiber composites reinforced with phenolic resin matrix surface preparation with plasma treatment.

Plasma surface treatment is regarded as an environmentally friendly process since no chemicals are involved and also as an effective way to modify the bondability and wettability of polymer surface by introducing polar groups without affecting the bulk properties [8, 9, 10]. Plasma surface treatment is often the preferred way to treat the surfaces as it offers more stable and long-lasting surface energy enhancement than any other treatments [11]. However, conventional plasma treatment has also negative aspects: it requires a low pressure (partial vacuum) and thus, the parts must be processed in a vacuum chamber, restricting the part size; the price of the setup is not negligible.

In this study, atmospheric pressure plasma has been used.

Plasmas operating at atmospheric pressure (AP) have found widespread commercial use as a tool for the pretreatment of polymers [12] .Atmospheric

pressure plasma has been developed to operate at near ambient temperature and atmospheric pressure eliminating the expensive vacuum systems [11,13]. AP are interesting alternative to other pretreatment methods (e.g. low-pressure plasma or wet chemical treatment) because of in-line process capabilities, relatively low costs, and low requirements on personal and environmental safety. Plasma has been created using three different gas mix (He, He with 1% O2, He with 1% N2). The wettability of the specimens was estimated both for untreated and plasma treated specimens through drop contact angle measurements.

Scanning electron microscopy was used to study the effect of atmospheric plasma treatment on the surface roughness of specimens.

The adhesion properties of the activated surfaces are evaluated by lap shear tests. Lap shear testing was carried out for bonded joints of all the three types of mixed gases plasmas in order to determine the joint strength.

1.1 State of art

In the last 40 years, plasma applications have been various, especially in welding and semiconductor production. Especially in this one, plasma is used for specific surface treatments with the aim of increase the wettability of the surface, activate it and cover it with a thin film. All of this is possible thanks to the great amount of active species present in the plasma that react with the surface, and thanks to the low temperature at which plasma can be created. Those plasmas, though, need vacuum setups, that

give the name of low-pressure plasmas. For sure, this aspect strongly limits the possible applications for many reasons. First of all, it's not possible to work with materials that don't stand high vacuum or that can be damaged by those pressures. Dimensions of objects that can be treated are limited by the vacuum chamber size, that can't be so big for economical and practical reasons. Lastly, the systems that generate and maintain vacuum pressures are typically expensive. This leaded plasma treatment to be used only for special applications with high interest, for example the production of some selected semiconductors.

Recently, the new system of plasma, called Atmospheric Pressure Plasma (APP), can supply innovative aspects that overcome the previous listed disadvantages, allowing a wide application of the plasma treatments. In particular, it can be used for cheaper applications, as it doesn't require vacuum systems. It's faster, because there is no insertion phase of the piece to be treated, and it can be used in in-line process.

APP treatments have been recent subjects for scientific researches during the last 10 years. It has been widely used to improve polymer coating, adhesion and painting, by the mechanism of cleaning surface and introducing polar groups (–COOH, –OH), thus increasing surface energy, wettability and adhesion capability without affecting bulk properties. For this reason, plasma treatment is considered to be able to modify a lot of types of surface and enhance surface energy, as it has been observed with for example glass, ABS, polycarbonate, polyolefins, or polyester, where APP is used to pretreat polyester fabric in order to provide an active surface for the ink jet printing.

Also, the preparation of hydrophobic film on glass surface can be carried out by this treatment type.

APP has been used to clean and activate polymeric surfaces for example by H.M.S. Iqbal, S. Bhowmik and R. Benedictus from the Faculty of Aerospace Engineering, Delft University of Technology, [23], during 2010. They investigated the effects of atmospheric pressure plasma treatment on the surface energy of polyetheretherketone (PEEK), carbon fibers (CF) and glass fiber (GF) reinforced polyphenylenesulfide (PPS). To study the effect of plasma treatment, all three materials were treated with atmospheric pressure plasma. Samples were plasma treated using TIGRES Plasma-BLASTER MEF equipment. It operates at 230V and 50/60HZ frequency.

So it can be seen that a multitude of materials can be treated by APP. With glass surface, for example, it has been seen [45] that contact angle values diminished upon the application of the preparation process, involving an improvement in surface energy. APPT (atmospheric pressure plasma torch) treatment not only promoted the cleaning of the surfaces, but also increased the amount of surface valleys due to plasma flux impact, thus improving adhesion. At a final glance, glass bonded with epoxy, silicone or cyanoacrylate did not show statistical differences in strength for the untreated adherent sand with APPT, in contrast with APPT glass–polyurethane adhesive bondings.

Previous studies have investigated the use of air plasmas for the activation of temperature sensitive polymers prior to adhesive bonding [27-29] and textile polymer treatment [30]. The effect of the plasma is to bombard the

surface with free radicals, electrons and ions resulting in the decomposition of organic molecules with lower-molecular-weight polymer chains that can vaporize off (ablate) from the surface.

Air is often used for plasma applications, as it's a natural part of our environment, and special attention is given in the last decades to the study of plasmas in air at atmospheric pressure and their applications.

Air is used especially to clean the surfaces. It has been used in the removal of a 5–8 nm thick layer of FreKote 710-NC, a widely used mold release agent, from composite material surface. [46] During that research, it has been seen that a 7% enhancement in lap-shear strength was achieved with the plasma treatment compared to grit blasting.

In literature we can find studies about atmospheric pressure plasmas using other gases, different from air. Those gases are introduced in the researches to try to increase the benefits of the treatments, using special characteristics of the molecules activated in the different situations.

Bowditch and Shaw [1] have revealed that when oxygen gas was used to modify polymer surfaces, it resulted in the most effective way to introduce the hydrophilicity to a polymer surface. Adhesion properties are also strongly influenced by the surface topology. It can be seen that APP can be used to treat polymeric fibers to increase the adhesion to epoxy resin to produce fiber reinforced materials.

Y. Ren, C. Wang and Y. Qiu [19] had found that the amount of oxygen added to the carrier gas helium has a significant influence on the APPJ treatment and the aging effect. The excited species of helium have relatively

long lifetime (1 ms to 1 s) known as metastable species at a high excitation energy of 19.8 eV to 20.6 eV, while oxygen molecules have ionization potential of 13.6 eV. Therefore, when a metastable helium atom collides with an oxygen molecule, the oxygen can be ionized because its ionization energy is lower than the excitation energy of metastable helium. The reaction can be described as follows: $He^* + O_2 \rightarrow O_2^+ + He + e^-$ which is known as Penning Ionization. With increasing O_2 content in the mixture, the density of helium metastables decreases due to Penning Ionization, transferring energy to oxygen species and other species with lower energy levels. Therefore, the excess presence of oxygen affects the density of helium metastables, which will influence the surface crossing linking. According to Schonhorn and Hansen [31], an inert gas discharge action can induce a so-called CASING (cross-linking by activated species of inert gases) process, creating a cross linked layer on the surface of the substrate. The formation of the cross linked layer on the polymer surface is critical for restricting the chain mobility and thus inhibiting the hydrophobic recovery after the plasma treatment. For various material processes with plasma, the reactive gases such as oxygen, nitrogen, and other gases are usually mixed into the carrier gas to provide chemically reactive species. In the APPJ (Atmospheric Pressure Plasma Jet) treatment, the amount of the oxygen gas influences the surface modification effectiveness and the aging process during the storage.

In the study of Choi and Kim [44], a new atmospheric pressure N_2 cold plasma torch has been developed by providing high voltage to the electrode via transformer with 60 Hz power supply. N_2 cold plasma torch ejects plasma

jets with high velocity having low gas temperature suitable to polymer treatments. Discharge characteristics of N_2 cold plasma are examined by current–voltage probe, optical emission spectroscopy and thermocouple. As one possible application, polypropylene surfaces are treated with N_2 cold plasmas for adhesion improvement, and discharge parameters are correlated with the degree of surface modification to explain mechanism responsible for the increased adhesion. Variations of the gas temperature with position of power electrode measured from 1 to 5 mm below ejection slit, are measured using thermocouple. Gas temperatures are maintained below 60° C, suitable to polymer treatment, having little dependency on distance from ejection slit. The gas temperature dependency on power electrode position is similar to that of power dissipation in discharge. After that, a lap shear test is conducted relating the strength with the position of the electrode (see the image below), resulting in an increase of the strength compared to untreated surface.

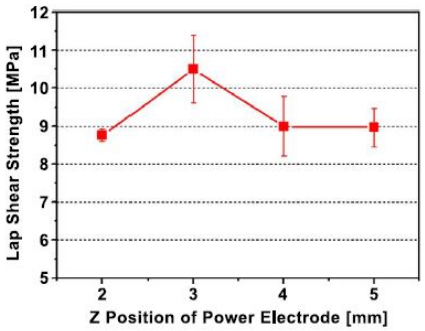

Figure 1.1: Choi and Kim results

Until now, there is no widespread use of Helium gas, the literature is quite

limited on this specific options/parameters.

The epoxy resin used in this study connects to the surface thanks to the ammine groups ($-NH_2$), so in order to increase this active groups, this present research focuses on Helium gas with added Nitrogen or Oxygen.

2 Experimental details

2.1 Materials

2.1.1 Epoxy resin

Epoxy resins, also known as polyepoxides, are a class of reactive prepolymers and polymers which contain epoxide groups. Epoxy resins may be reacted (cross-linked) either with themselves through catalytic homopolymerisation, or with a wide range of co-reactants including polyfunctional amines, acids (and acid anhydrides), phenols, alcohols, and thiols. These co-reactants are often referred to as hardeners or curatives, and the cross-linking reaction is commonly referred to as curing. Reaction of polyepoxides with themselves or with polyfunctional hardeners forms a thermosetting polymer, often with strong mechanical properties as well as high temperature and chemical resistance.

Epoxy has a wide range of industrial applications, including metal coatings, use in electronic and electrical components, high tension electrical insulators, fiber-reinforced plastic materials, and adhesives.

Epoxy adhesives are a major part of the class of adhesives called "structural adhesives" or "engineering adhesives".

Many current aerospace design for stringer-to-skin assemblies utilized in fuselage, horizontal and vertical stabilizers typically use film adhesive for bonding.

Epoxy resins typically require a precise mix of two components which

form a third chemical. Depending on the properties required, the ratio may be anything from 1:1 or over 10:1, but in every case they must be mixed in exactly the right proportions, and thoroughly to avoid unmixed portions. The final product is then a precise thermo-setting plastic. Until they are mixed the two elements are relatively inert, although the 'hardeners' tend to be more chemically active and should be protected from the atmosphere and moisture.

The following research employs epoxy resins Hysol© EA9380 and Hysol© EA9394 , that are a low temperature curing two component assembly pastes, that can be applied for structural bonding using a manual mixing or a dual cartridge static mixer kit.

Uncured Adhesive Properties

	Part A	Part B	Mixed
Color	Black	White	Grey
Mix Ratio			
by volume	100	50	
by weight	100	55	
Density, mixed g/cc	0.97	0.99	0.974
Viscosity, Poise/Pa.s @ 85°F/30°C (1)	1,800/180	2,150/215	1.,600/160
Working Life @ 75°F, hours (2)			3
Surface Carbonation			None

Table 2.1: Physical characteristics of components Hysol© EA9380

Hysol© EA9380

Component A of Hysol© EA9380 The composition of first component is[1]

[1]CAS number = Chemical Abstracts Service

Hazardous components	CAS NUMBER	%
Polyfunctional epoxy resin	Proprietary	30 - 60
Epoxy resin	Proprietary	30 - 60
Epoxy acrylate oligomer	Unknown	10 - 30
Synthetic rubber	Proprietary	1 - 5
Treated fumed silica	67762-90-7	1 - 5

Table 2.2: Component A

The physical state is liquid, black colored, very viscous at room temperature.

Component B of Hysol© EA9380 The composition of second component is

Hazardous components	CAS NUMBER	%
2,2'-Dimethyl-4,4'-methylenebis(cyclohexylamine)	6864-37-5	60 - 100
Silica, amorphous, fumed, crystal-free	112945-52-5	5 - 10
Titanium dioxide	13463-67-7	0.1 - 1

Table 2.3: Component B

The physical state is liquid, white colored, less viscous at room temperature than component A. It contains amines.

Uncured Adhesive Properties

	Part A	Part B	Mixed
Color	Gray	Black	Gray
Viscosity, 77°F	4000-8000 Poise	200-700 Poise	1600 Poise
Brookfield, HBT	Spdl 7 @ 20 rpm	Spdl 4 @ 20 rpm	Spdl 5 @ 20 rpm
Viscosity, 25°C	400-800 Pa·S	20-70 Pa·S	160 Pa·S
Brookfield, HBT	Spdl 7 @ 2.09 rad/sec	Spdl 4 @ 2.09 rad/sec	Spdl 5 @ 2.09 rad/sec
Density (g/ml)	1.50	1.00	1.36

Table 2.4: Physical characteristics of components Hysol© EA9394

Hysol© EA9394

Component A of Hysol© EA9394 The composition of first component is

Hazardous Component(s)	CAS Number	Percentage*
Aluminum	7429-90-5	30 - 60
Tetraglycidyl diaminodiphenylmethane	28768-32-3	30 - 60
Epoxy resin	Proprietary	10 - 30
Modified epoxy resin	Unknown	5 - 10
Treated fumed silica	67762-90-7	1 - 5

Table 2.5: Component A

Component B of Hysol© EA9394 The composition of second component is

Hazardous Component(s)	CAS Number	Percentage*
Tetraethylene pentamine	112-57-2	30 - 60
Substituted piperazine	Proprietary	30 - 60
Silica, amorphous, fumed, crystal-free	112945-52-5	5 - 10
Triethylenetetramine	112-24-3	1 - 5
Carbon black	1333-86-4	0.1 - 1

Table 2.6: Component B

2.2 Epoxy optimization

This products requires mixing two components together just prior to application to the parts to be bonded. Complete mixing is necessary. The temperature of the separate components prior to mixing is not critical, but should be close to room temperature (25°C). [2]

The mixing ratio between the two components is, by weight:

- component A = 100, component B = 55 for Hysol© EA9380
- component A = 100, component B = 17 for Hysol© EA9394

[2]Hysol EA 9380 Henkel Corporation Aerospace Group Guide

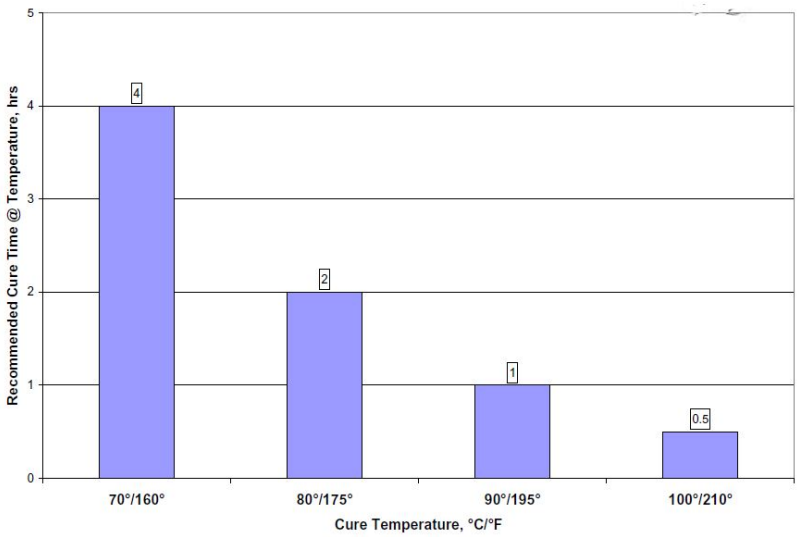

Figure 2.1: Curing time suggestions

Application Samples have been created by spreading the mixed components in layers of 1 mm thickness on aluminum foil, resulting in about 6 cm^2. In some trials the temperature of the mixed has been slightly increased (35°C) to facilitate and to regularize the spreading procedure.

Curing Curing may be done at temperature at 70°C or above. As suggested in the preparation guide, all the samples have been cured at a temperature of 80°C for 120 minutes. This, as can be seen in literature, enhances shear stress resistance, as well as it reduces metal-metal peeling.[3]

Problems The mixing procedure is a very delicate process: during the hand movements in open container, air bubbles are trapped into the mixture,

[3]Henkel© Corporation

with the risk of giving a foam shaped cured epoxy. During the first period of research, without a mixing kit, a method to efficiently remove air bubbles has been searched, before the curing session.

Vacuum degas Vacuum degassing involves actual removal of the air surrounding the epoxy by allowing the air that is trapped within the epoxy to easily escape.[4]

To do this, samples have been put in a desiccator, allowing all the upper surface of the sample to be vacuumed. A little "rise" in the volume of epoxy has been observed once the material is subjected to the vacuum.

The pumps used can reach -60 kPa in 2 minutes (pump A) or 30 seconds (pump B).

Test have been conducted maintaining constant vacuum value, changing time of permanence of the sample in the dedicator.

As we can see in the results, vacuum should be held for as short a period of time as possible without pulling too much vacuum, otherwise a counter-productive phenomenon can happen, creating more bubbles in the epoxy.

Heating Heating is an efficient and the simplest method to remove bubbles from epoxy. The key to this technique is to keep the product in a wide container that has large amounts of epoxy in the X and Y dimension, but little in the Z dimension. This gives the maximum amount of surface area for the bubbles to escape.

[4]www.epotek.com Tech Tips

In our experiment, the sample is 1±0.5 mm thick, and 2×3 cm wide, it has been placed on a copper plate, heated with 2 cartridge type resistors of 120 W power.

Combinations Several attempts have been made to find the best solution at our first problem, the air bubble presence in the cured epoxy. Combining the two degassing method previously illustrated, the research followed the suggestions of Epotek©, trying to implement the results.

These are the combinations of the various samples:

Table 2.7: Epoxy treating combinations

Sample	Vacuum (-60 kPa) time (minutes)	Heating temperature (°C)	Heating time (minutes)
1	none	none	none
2	5	none	none
3	10	none	none
4	none	none	none
5	30	none	none
6	none	34±1	10
7	5	34±1	5
8	10	34±1	10
9	30	34±1	30
10	none	none (heated before application)	none
11	none	40	10
12	none	40	15
13	none	40	20

Samples 1, 4 and 10 didn't follow the ideal combination, but have different curing times or, for the sample 10, has been heated before application.

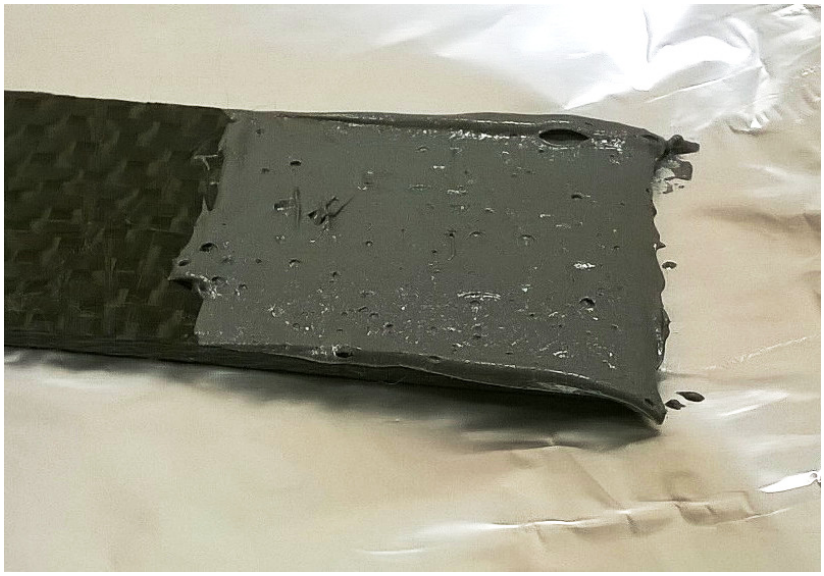

Figure 2.2: Epoxy resin on a carbon fiber plate after heat and vacuum treatment. Note the bubbles that come up to the surface

Measurements The performance of the degassing process has been quantified by counting the number of bubbles, their diameters, therefore their areas, using microscope images. The magnification of the images is 5×. The considered cross section area is a selected 700×700 pixel square. It has been calculated that, at magnitude 5×,

$$0.5mm = 450px$$

It follows that, considering a circle,

$$Area_{px^2} = \frac{\pi * d_{px^2}^2}{4} = \frac{\pi * d_{mm^2}^2 * 810000}{4}$$

from there it can be easily calculated the equivalent area diameter in mm.

Sample preparation To obtain a proper cross section to analyze, the samples have been cut manually using either a box cutter either a sharp blade. This last method resulted more precise because of the setting of the cut.

Then cross sections have been polished with glass-paper 1200# grit. This simplified the image analysis, because the cut bubbles, filled with tiny glass particles, have an homogeneous color and texture.

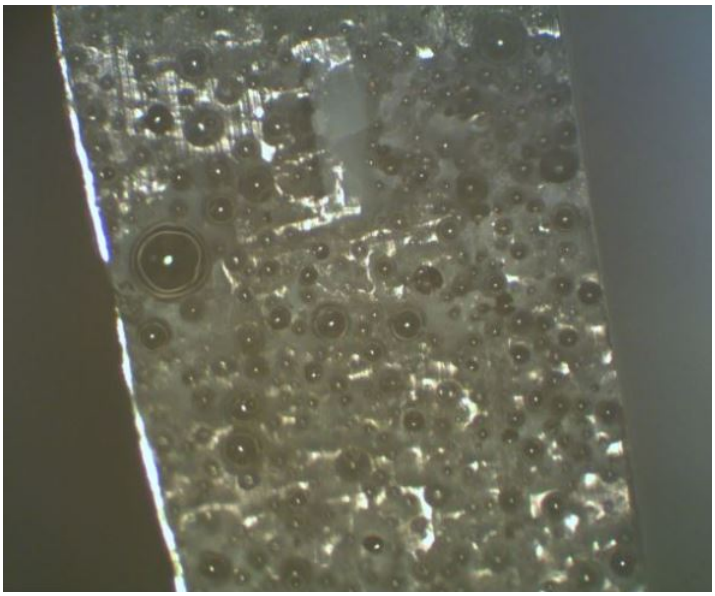

Figure 2.3: cut cross section

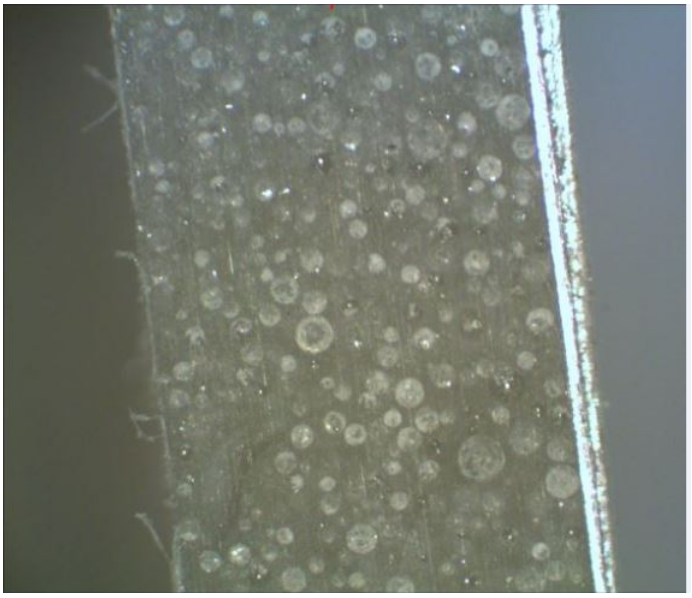

Figure 2.4: Glass-papered cross section.Note the homogeneous texture of the bubbles

Software The image analyzer software used is ImageJ.

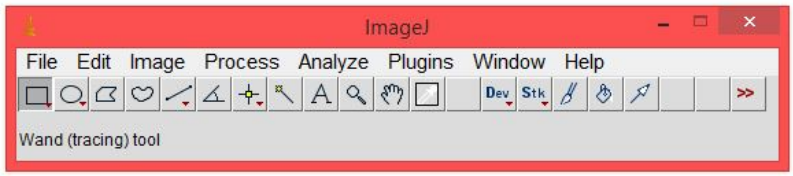

Figure 2.5: ImageJ software

ImageJ is a public domain, Java-based image processing program developed at the National Institutes of Health. ImageJ was designed with an open architecture that provides extensibility via Java plugins and recordable macros. Custom acquisition, analysis and processing plugins can be developed using ImageJ's built-in editor and a Java compiler. User-written plugins

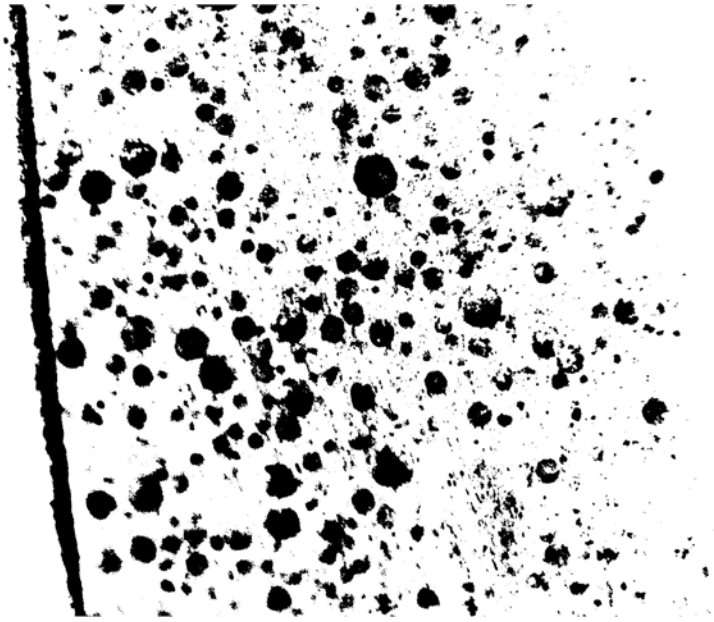

Figure 2.6: Processed image

make it possible to solve many image processing and analysis problems.[5]

After processing the image with contrast, brightness and threshold settings, the command *Analyze* $\rightarrow$ *Analyze particles* selects areas and draws a contour around each bubbles, measuring its area in px^2.

[5]http://en.wikipedia.org/wiki/ImageJ

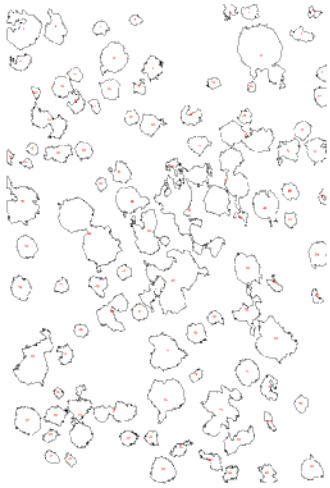

Figure 2.7: Analyze particles

Analyze particles give a results in the form of Excel© file with informations of Label, Area, Mean, Mode, Min, Max, Circ., IntDen, RawIntDen, AR, Round and Solidity. The research focuses mostly on the area and the number of the bubbles, trying to minimize the total area.

Table 2.8: Example of result

	A	B	C	D	E	F	G	H	I	J	K	L	M
1		Label	Area	Mean	Mode	Min	Max	Circ.	IntDen	RawIntDe	AR	Round	Solidity
2	1	9.5x.bmp	1524	249.478	255	0	255	0.229	380205	380205	1.600	0.625	0.736
3	2	9.5x.bmp	1191	249.647	255	0	255	0.658	297330	297330	1.057	0.946	0.900
4	3	9.5x.bmp	755	241.152	255	0	255	0.115	182070	182070	1.140	0.878	0.600
5	4	9.5x.bmp	602	248.646	255	0	255	0.176	149685	149685	1.604	0.624	0.546
6	5	9.5x.bmp	1345	253.673	255	0	255	0.444	341190	341190	1.181	0.847	0.844
7	6	9.5x.bmp	1370	254.255	255	0	255	0.273	348330	348330	1.825	0.548	0.775
8	7	9.5x.bmp	636	252.193	255	0	255	0.153	160395	160395	1.279	0.782	0.551
9	8	9.5x.bmp	698	255	255	255	255	0.346	177990	177990	2.019	0.495	0.734
10	9	9.5x.bmp	2067	249.448	255	0	255	0.140	515610	515610	1.868	0.535	0.622
11	10	9.5x.bmp	2127	251.883	255	0	255	0.381	535755	535755	1.059	0.944	0.788
12	11	9.5x.bmp	1312	253.834	255	0	255	0.325	333030	333030	1.246	0.803	0.766
13	12	9.5x.bmp	2019	232.645	255	0	255	0.240	469710	469710	1.258	0.795	0.762
14	13	9.5x.bmp	683	252.760	255	0	255	0.122	172635	172635	2.241	0.446	0.535
15	14	9.5x.bmp	3949	250.415	255	0	255	0.095	988890	988890	2.068	0.484	0.582
16	15	9.5x.bmp	1793	251.302	255	0	255	0.216	450585	450585	1.785	0.560	0.722
17	16	9.5x.bmp	3275	252.119	255	0	255	0.407	825690	825690	1.144	0.874	0.874
18	17	9.5x.bmp	947	253.654	255	0	255	0.279	240210	240210	2.181	0.458	0.648
19	18	9.5x.bmp	402	248.022	255	0	255	0.415	99705	99705	1.288	0.776	0.762

2.2.1 Carbon fiber plates

Carbon fiber, alternatively graphite fiber or CF, is a material consisting of fibers about 5–10 μm in diameter and composed mostly of carbon atoms.

To produce carbon fiber, the carbon atoms are bonded together in crystals that are more or less aligned parallel to the long axis of the fiber as the crystal alignment gives the fiber high strength-to-volume ratio. Several thousand carbon fibers are bundled together to form a tow, which may be used by itself or woven into a fabric.

The properties of carbon fibers, such as high stiffness, high tensile strength, low weight, high chemical resistance, high temperature tolerance and low thermal expansion, make them very popular in aerospace, civil engineering, military, and motorsports. However, they are relatively expensive when compared to similar fibers, such as glass fibers or plastic fibers.

Carbon fibers are usually combined with other materials to form a composite. When combined with a plastic resin and wound or molded it forms carbon fiber reinforced polymer (CFRP, often referred to as carbon fiber) which has a very high strength-to-weight ratio, and is extremely rigid although somewhat brittle.

The binding polymer is often a thermoset resin such as epoxy, but other thermoset or thermoplastic polymers, such as polyester, vinyl ester or nylon, are sometimes used. The composite may contain other fibers, such as aramid (e.g. Kevlar, Twaron), aluminum, ultra-high-molecular-weight polyethylene (UHMWPE) or glass fibers, as well as carbon fiber. The properties of the

final CFRP product can also be affected by the type of additives introduced to the binding matrix (the resin).

The reinforcement will give the CFRP its strength and rigidity; measured by stress and elastic modulus respectively. Unlike isotropic materials like steel and aluminum, CFRP has directional strength properties. The properties of CFRP depend on the layouts of the carbon fiber and the proportion of the carbon fibers relative to the polymer.

During this research, carbon fiber composites reinforced with phenolic resin matrix plates have been treated with atmospheric pressure plasma to understand the changes in the nature of the surface and to increase the bond strength with epoxy resin.

2.3 Atmospheric plasma treatment

Plasma is a chemical active media, consisting of ionized gas. It is the fourth state of matter (plasma, liquid, solid, gas) and is present in more than 99% of the universe.

It's composed by electrons, ions and neutrals, which are in fundamental and excited state. Macroscopically it is electrically neutral, but because of his nature, it contains free charge carrier and is electrically conductive.

A plasma is created by applying energy to a gas [32] in order to reorganize the electronic structure of the species (atoms, molecules) and to produce excited species and ions. This energy can be thermal, or carried by either an electric current or electromagnetic radiations. [33]

The atmospheric plasmas are generated from electrical energy. The electric field transmits energy to the gas electrons (which are the most mobile charged species). This electronic energy is then transmitted to the neutral species by collisions. These collisions [34] follow probabilistic laws and can be divided in:

- Elastic collisions: they do not change the internal energy of the neutral species but slightly rise their kinetic energy
- Inelastic collisions: when electronic energy is high enough, the collisions modify the electronic structure of the neutral species. It results in the creation of excited species or ions if the collisions are energetic enough.

Most of the excited species have a very short lifetime and they get to ground state by emitting a photon. The "metastable species" are also excited states but with a long lifetime because their decay by emission of radiation is hampered as there are no allowed transitions departing from the respective state: decay can only take place by energy transfers through collisions.

Plasmas classification Depending on the type of energy supply and the amounts of energy transferred to the plasma, the properties of the plasma change, in terms of electronic density or temperature. These two parameters distinguish plasmas into different categories, presented in the figure below:

The atmospheric plasma sources described are supposed to be positioned near the glow discharges and the arcs.

In this classification, a distinction can be made between:

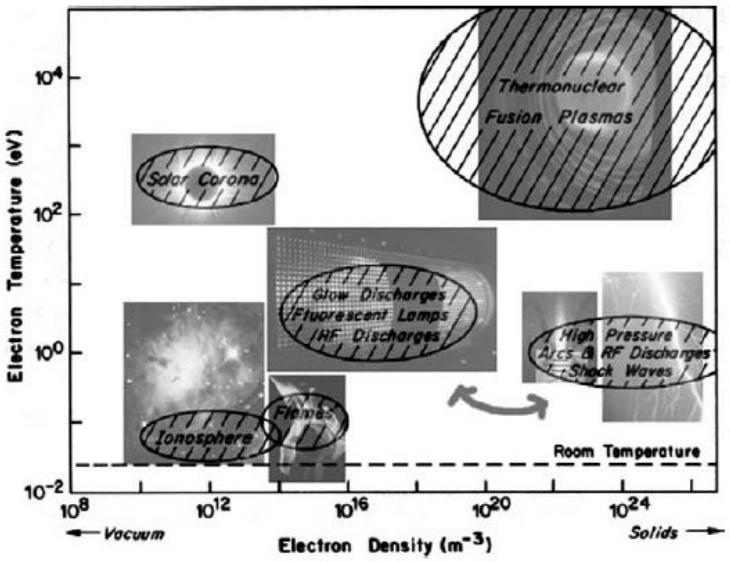

Figure 2.8: Plasma categories

- Local thermodynamic (or thermal) equilibrium plasmas (LTE)
- Non-local thermodynamic equilibrium plasmas (non-LTE).

Atmospheric pressure plasmas: LTE or non-LTE? The Local Thermodynamic Equilibrium notion [35] is really important, especially for a spectroscopic study of the plasma, since the determination of the plasma parameters (particles distribution functions; electron, excitation, vibration temperatures...) is based on relationships which differ for plasmas in LTE or not.

LTE plasmas LTE plasma requires that transitions and chemical reactions are governed by collisions and not by radiative processes. Moreover,

collision phenomena have to be micro-reversible. It means that each kind of collision must be balanced by its inverse (excitation/deexcitation; ionization/recombination; kinetic balance) [36]. Moreover LTE requires that local gradients of plasma properties (temperature, density, thermal conductivity) are low enough to let a particle in the plasma reach the equilibrium: diffusion time must be similar or higher than the time the particle need to reach the equilibrium [37]. For LTE plasma, the heavy particles temperature is closed to the electrons temperature (ex: fusion plasmas). According to the Griem criterion [38], an optically thin homogeneous plasma is LTE if the electron density fulfills:

$$n_e = 9.10^{23}(\frac{E_{21}}{E_{H^+}})(\frac{kT}{E_{H^+}}) \qquad (m^{-3})$$

where

- E_{21} represents the energy gap between the ground state and the first excited level,
- E_{H^+}=13.58 eV is the ionization energy of the hydrogen atom,
- T is the plasma temperature.

This criterion shows the strong link that exists between the required electron density for LTE and the energy of the first excited state. Those rules for LTE are very strict. Thus most of the plasmas deviate from LTE, especially all types of low density plasma in laboratories.

Non-LTE plasmas Departure from Boltzmann distribution for the density of excited atoms can explain the deviation from LTE. Indeed, for low-lying levels, the electron-induced deexcitation rate of the atom is generally lower than the corresponding electron induced excitation rate because of a significant radiative deexcitation rate [36]. Another deviation from LTE is induced by the mass difference between electrons and heavy particles. Electrons move very fast whereas heavy particles can be considered static: electrons are thus likely to govern collisions and transitions phenomena. Deviations from LTE are also due to strong gradients in the plasma and the associated diffusion effects. It has been shown that the LTE distribution can be partial. For example, LTE can be verified for the levels close to ionization threshold [39] (e.g., 5p levels and higher, in argon plasma): such plasmas are pLTE (partial LTE). The non-LTE plasmas can be described by a two temperature model: an electron temperature (T_e) and a heavy particle temperature (T_h). Regarding the huge mass difference between electrons and heavy particles, the plasma temperature (or gas temperature) is fixed by T_h. The higher the departure from LTE, the higher the difference between T_e and T_h is. More details on LTE and deviations from LTE are developed in the books by Huddlestone and Leonard [40], Griem [41], Lochte-Holtgreven [42] and Mitchner and Kruger [43].

Atmospheric pressure plasmas The figure below shows the influence of the pressure on the transition from a glow discharge (T_e>T_h) to an arc discharge.

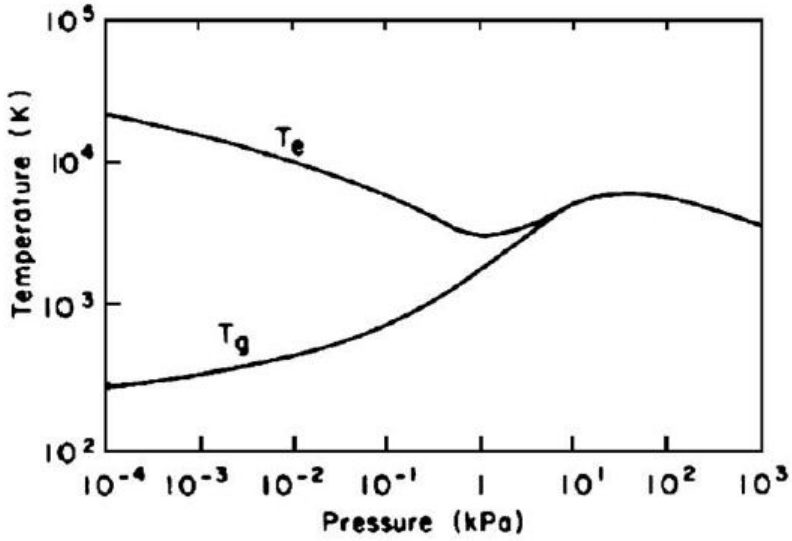

Figure 2.9: Influence of the pressure

Low pressure plasmas (10^{-4} to 10^{-2} kPa) are non-LTE. Heavy particles temperature is lower than the electronic one. The inelastic collisions between electrons and heavy particles are excitative or ionizing. These collisions do not rise the heavy particles temperature. When the pressure becomes higher, collisions intensify. They induce both plasma chemistry (by inelastic collisions) and heavy particles heating (by elastic collisions). The difference between T_e and T_h is reduced: plasma state becomes closer to LTE but does not reach it. The significant gradient of properties in plasma restricts a particle, moving in the discharge, achieving equilibrium. The density of the feeding power influences a lot the plasma state (LTE or not). On the whole, a high power density induces LTE plasmas (e.g. arc plasmas) whereas non-LTE plasmas are favored by either a low density of feeding power or a

pulsed power supply. In this latter case, the short pulse duration prevents the equilibrium state from establishing. Finally, it is important to note that an atmospheric plasma jet can be divided in two zones:

- a central zone or plasma core which is LTE
- a peripheral zone which is non-LTE.

A classification with the different types of equilibrium is not really immediate and convenient to use. It's preferable to make an overview of various atmospheric plasma sources.

Atmospheric plasma sources The excitation frequency is important since it influences the behavior of the electrons and the ions. The atmospheric plasma sources can be classified regarding their excitation mode. Three groups are then highlighted:

- the DC (direct current) and low frequency discharges;
- the plasmas which are ignited by radio frequency waves (RF);
- the microwave discharges.

The trend of miniaturization of plasma systems is important in order to create low-powered directive portable systems and to reduce instrument and operation costs.

During the study, a atmospheric pressure RF plasma has been used. It doesn't require some expensive facilities of low-pressure plasmas, as vacuum

equipment. The dimensions of the setup are also reduced in comparison to industrial setups.

In the lab, a 20 V potential difference is applied, with a 1 A current (AC), for a 20 W average power, giving a 300 K plasma flame.

The current is given by a pulsed wave (about 6 kHz frequency), and the pulse width and duty cycle are set in order to get maximum power transferred to the gas.

The plasma setup is a dielectric breakdown system. A discharge in the gas is started applying a voltage between the electrodes (the voltage value depends on the values of gas pressure and the gap between the electrodes).

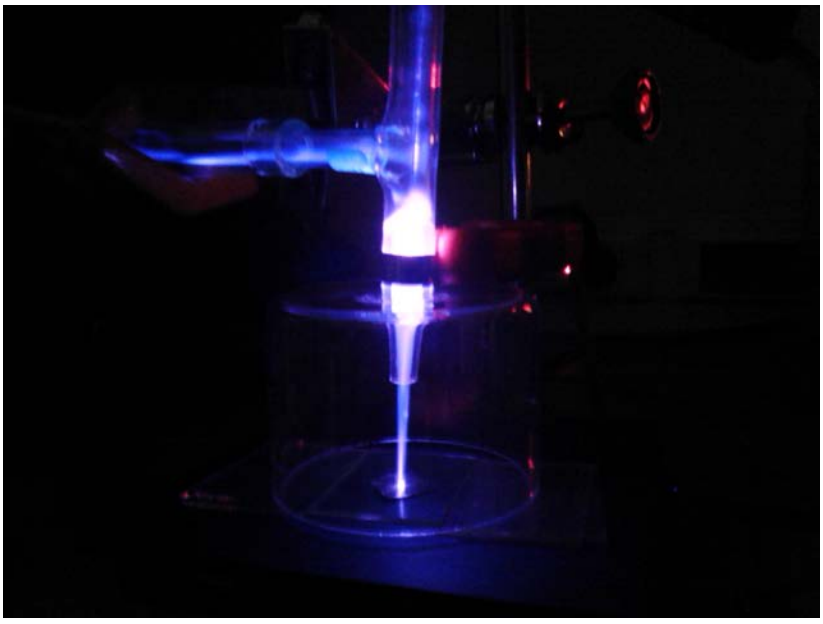

Figure 2.10: Plasma gun operating

Atmospheric plasma has various applications: cleaning, etching, coating. With the treatment used in this research, the aim is to clean the surface,

increase the surface energy (decrease the contact angle) and generate surface functional groups that will allow the epoxy resin to stick to the surface, with higher adherence properties. This is possible because plasma is a high chemically reactive media: high energy protons and high energy atoms ($^3He^*$, metastable triplet state helium) collide with the surface, with the creation of radicals. Those react with O_2, N_2 and H_2O creating $-OH$ and $-NH_2$ groups on the surface.

The surface activation (or functionalization) needed is the one that increases O and N groups, and that decreases F groups (fluorides).

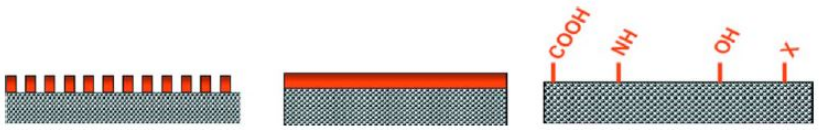

Figure 2.11: Surface treatment with plasma: etching, coating and surface functionalization

The treatment efficiency can be measured via drop contact angle and via XPS, so that the spectroscopic analysis can link the surface energy evolution to the surface composition and chemical bounds.

It has been observed, trough the contact angle measurement, that the surface activation remains stable over a quite long period (10 hrs).

Surface etching Surface etching consists in removing material from the treated sample surface in order to create a relief.

The etching rate depends on several parameters: plasma composition

(oxygen species), substrate nature, working conditions (power, gas flow, substrate position).

We'll see in the results that a particular molecule (SiO_2) becomes more present in the surface as the treatment last longer. This is probably due to surface etching by the plasma flow. Silica is in effect a component of the CFRP as an additive, to define the mechanical properties of the composite material.

Plasma treatment The plasma treatment conducted for the measurement consists, as already said, in a fixed plasma flow blowing to the center of a square plate area.

Treatment is now required to a larger surface, in order to prepare samples for the shear tests, so it's necessary to scan the surface with the plasma flow. For this purpose, a program has been written using the software LabVIEW© from NationalInstruments.

Two ThorLab© stepper motors are connected to a movable platform, allowing a controlled 2D movement of the surface under the plasma flow.

The path that has been followed is shown here:

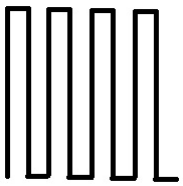

Figure 2.12: Path of scanning

The treated area has been always 25mm ×25mm.

After the treatment, the epoxy glue has been spread on the surface, and two plates of carbon fibers have been glued together, following the chosen process to minimize air bubbles and cure. The prepared samples have then been tested with single-lap shear test.

The scans test have been conducted with different gaps between the lines. The parameters are:

First scan

- scan rate: 0.5 mm/s
- gap between lines: 2.5 mm
- plasma beam diameter: 1 mm

Second scan

- scan rate: 0.5 mm/s
- gap between lines: 1.5 mm
- plasma beam diameter: 1 mm

The second scan has been conducted twice with two different plasma jets to investigate the different effects that can be obtained: kHz beam and RF (Radio Frequencies) beam.

Spectrum lines of plasma To obtain always the same characteristics of the plasma, spectrum lines have been monitored, after having set the parameters as follows:

- current pulse: 6.7 kHz
- duty cycle: 15.2 % (pulse width: 22.7 μs)

The spectrum of the plasma has been monitored with a spectrometer

Table 2.9: Spectrum Lines

Ion	Observed Wavelength Vac (nm)	Ritz Wavelength Vac (nm)	Aki (s-1)	Lower Level Conf., Term, J	Upper Level Conf., Term, J
He I	706.5190	706.521530	9.284e+06	1s2p 3P° 1	1s3s 3S 1
O I	777.194	777.1944	3.69e+07	2s22p3(4S°)3s 5S° 2	2s22p3(4S°)3p 5P 3

2.4 Contact angle measurements

Drop shape analysis is a good way to measure contact angles helping in understanding wetting of materials and adhesion properties.

The set up requires a syringe connected to a needle above the surface; a water drop of the precise volume of 2 μl is sent by a special pump, then the drop is put in contact with the surface; the adhesion of liquid to the surface makes the drop stay on the surface.

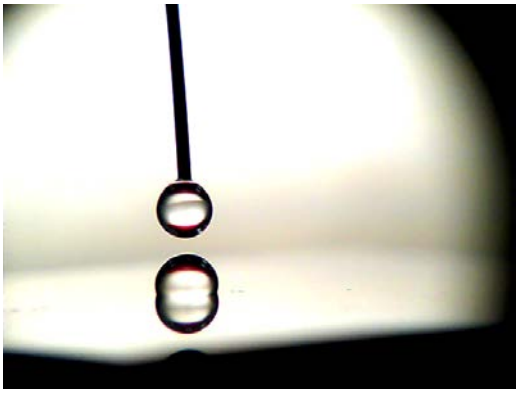

Figure 2.13: Drop on needle and on surface

Assuming that the drop of water on the surface is symmetric, this method view the still image of the shape that is the result of interfacial tension and gravity between the drop and the surface. The interface is called liquid-solid-vapor LSV, that can be understood looking at the following image:

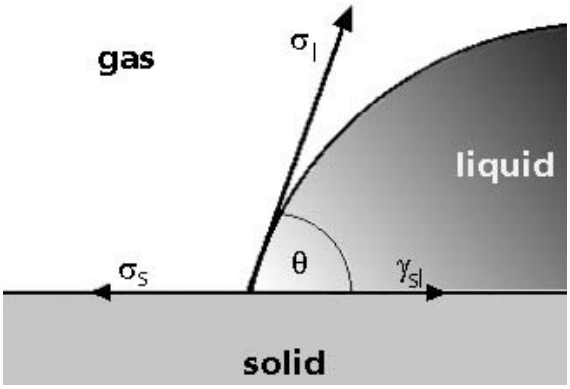

Figure 2.14: LSV interface

The image is taken by a macro camera staring horizontally or at most 3° above the horizon. This requires proper lighting and camera angle. Even more importantly, it demands finding the baseline accurately, which is the

difficult part of contact angle measurements. The accuracy of the measurement is about $\pm 1°$.

Contact angle is then measured by fitting the profile of the drop using mathematical expression and calculating the slope of the tangent to the drop at the interface line.

Software The software used is ImageJ again. The specific part of drop analysis is done with the DropSnake[6] and with LB-ADSA (Low Bond Axisymmetric Drop Shape Analysis)[7] plugins. They are based on B-spline snake which in reason of their elasticity unify the aspects of locality of the contact angle to the guidance provided by the global drop contour, analytically solving the Young-Laplace equation according to photographic images of axisymmetric sessile drops.

2.5 SEM

A scanning electron microscope (SEM) is a type of electron microscope that produces images of a sample by scanning it with a focused beam of electrons. The electrons interact with atoms in the sample, producing several signals (secondary electrons (SE), back-scattered electrons (BSE), characteristic X-rays, light (cathodoluminescence) (CL), specimen current and transmitted electrons) that can be detected and that contain informations about the sample's surface topography and composition.

[6]http://www.epfl.ch/publications/stalder0601.html
[7]http://www.epfl.ch/publications/stalder1001.html

The electron beam is generally scanned in a raster scan pattern, and the beam's position is combined with the detected signal to produce an image.

SEM can achieve resolution better than 1 nanometer. Due to the very narrow electron beam, SEM micrographs have a large depth of field yielding a characteristic three-dimensional appearance useful for understanding the surface structure of a sample.

Specimens can be observed in high vacuum, in low vacuum, in dry conditions (in environmental SEM), and at a wide range of cryogenic or elevated temperatures, but normally, conventional SEM requires samples to be imaged under vacuum, because a gas atmosphere rapidly spreads and attenuates electron beams.

The most common mode of detection is by secondary electrons emitted by atoms excited by the electron beam. On a flat surface, as in our case, the plume of secondary electrons is mostly contained by the sample. By scanning the sample and detecting the secondary electrons, an image displaying the topography of the surface is created. Since the detector is not a camera, there is no diffraction limit for resolution as in optical microscopes and telescopes.

For conventional imaging in the SEM, specimens must be electrically conductive, at least at the surface, and electrically grounded to prevent the accumulation of electrostatic charge at the surface. Non conductive specimens tend to charge when scanned by the electron beam, and especially in secondary electron imaging mode, this causes scanning faults and other image artifacts. This is the case of the samples analyzed during the research, being made of polymeric matter.

Images have been taken with both the BSE and the SE detectors, using low current to limit the charge effect.

- Backscattered electrons (BSE) consist of high-energy electrons originating in the electron beam, that are reflected or back-scattered out of the specimen interaction volume by elastic scattering interactions with specimen atoms. Since heavy elements (high atomic number) backscatter electrons more strongly than light elements (low atomic number), and thus appear brighter in the image, BSE are used to detect contrast between areas with different chemical compositions.

- The most common imaging mode collects low-energy (<50 eV) secondary electrons that are ejected from the k-shell of the specimen atoms by inelastic scattering interactions with beam electrons. Due to their low energy, these electrons originate within a few nanometers from the sample surface. The brightness of the signal depends on the number of secondary electrons reaching the detector. If the beam enters the sample perpendicular to the surface, then the activated region is uniform about the axis of the beam and a certain number of electrons "escape" from within the sample. As the angle of incidence increases, the "escape" distance of one side of the beam will decrease, and more secondary electrons will be emitted. Thus steep surfaces and edges tend to be brighter than flat surfaces, which results in images with a well-defined, three-dimensional appearance.

2.6 FTIR (Fourier Transform InfraRed Spectroscopy)

The basis of infra-red spectroscopy is the vibrational excitation of molecules by the absorption of infra-red radiation (wavelength 1-100 μm). This occurs at characteristic photon energies, enabling structural analysis. Infrared spectroscopy can result in a positive identification (qualitative analysis) of every different kind of material. In addition, the size of the peaks in the spectrum is a direct indication of the amount of material present.

IR spectroscopy is normally performed in transmission mode, i.e. radiation is passed through the sample. This is a bulk technique, inappropriate for detecting surface change.

A more surface sensitive method is attenuated total reflectance Fourier transform infra-red spectroscopy (ATR-FTIR). Here the sample is held in intimate contact with an IR transparent crystal (e.g. KRS-5 or diamond) into which infra-red radiation is directed. The difference in refractive indices between the optically dense crystal and the sample result in internal reflection at their interface. However, the beam is not completely reflected at this junction: some propagates a short way into the sample, where it can excite vibrations and be absorbed. The penetration of this phenomena is dependent upon the incident wavelength but is typically about 0.1 - 10 μm.

2.7 XPS

X-ray Photoelectron Spectroscopy (XPS) is a technique that allows the investigation of the chemical composition of surfaces.

Using photoelectric effect, XPS identifies the elements near the surface and the surface composition, local chemical environment, probing the uppermost 5-8 nm of the sample.

UHV (Ultra High Vacuum; $p < 10^{-9} mbar$) is required in order to minimize the sample contamination and prevent scatter of the photoelectrons prior to analysis.

In an XPS experiment the sample is irradiated by high energy photons (typically soft X-rays) resulting in the ejection of core electrons by the photoelectron effect. The kinetic energies of these electrons are measured and their binding energies calculated. Binding energies are unique for every element, enabling the definition of the composition of the material.

The carbon fiber plate has been analyzed through XPS before and after the treatments, to investigate the changes in surface composition, that can help to reach the goal of maximize the wettability of the plate. Spectra have been obtained from the instrument: they exhibit a range of oxidation states, that often appear like a complex envelopes which can be deconvoluted using, for instance, the software Thermo Scientific™ Avantage Data System[8]. In order to quantify chemical states from overlapping peaks it is necessary to fit the data with synthetic peak shapes, to deconvolute into their components.

The investigation has been conducted selecting the target among the chemical species and elements we expect to be found. These are: C(1s): F(1s): N(1s): 0(1s): Si(2p).

[8]http://www.thermoscientific.com/en/product/avantage-data-system.html

2.8 Mechanical setup

The epoxy resin, as already explained in the previous parts, needs mixing of the two components. To do this faster and in a larger scale, a specific syringe (mixing kit) has been used.

The mixing kit from Henkel© is composed of two syringes stuck together of different diameters to ensure the proper mixing ratio of the two resin components, and a nozzle that mix the materials.

A mechanical setup to squeeze the syringe has been built *ad hoc*, as it can be seen in the photo below:

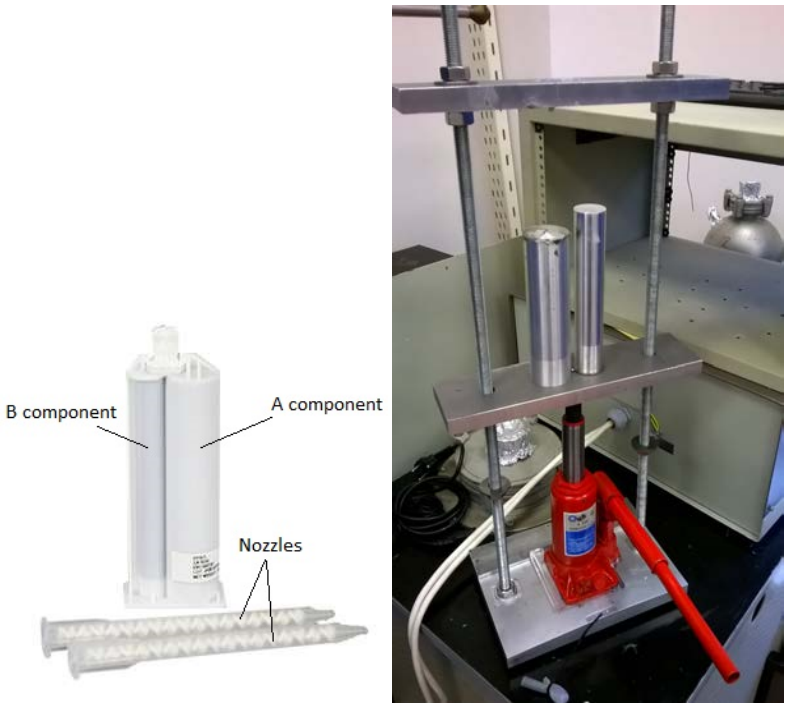

Figure 2.15: Syringe, nozzles and mechanical setup

2.9 Shear test

The conducted tests are of the type of Single-Lap Shear Test: despite all its obvious weaknesses, the lap-shear test is the most widely used method for producing in-situ shear strength data of an adhesively bonded joint.

The test consists essentially of two rectangular sections, typically 25 mm wide, 100 mm long and 1.6 mm thick, bonded together, with an overlap length of 25 mm.

Figure 2.16: Single-Lap Joint

3 Results

3.1 Drop Contact Angle - Epoxy

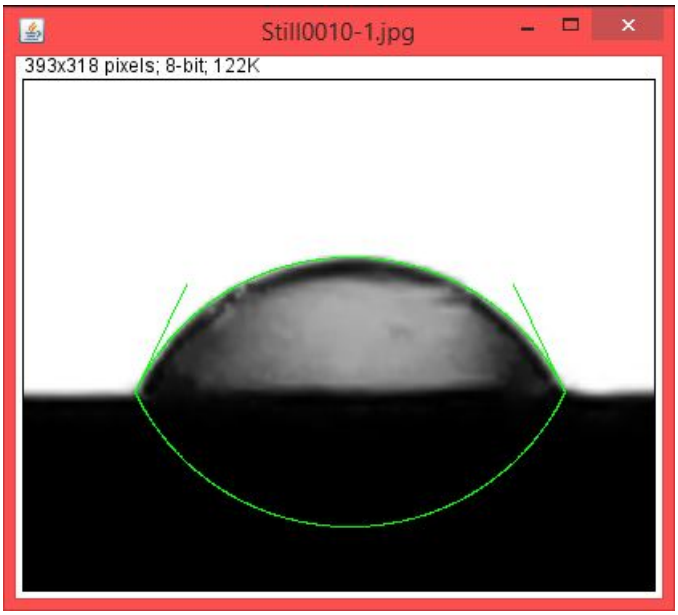

Figure 3.1: Drop on epoxy

The contact angles have been measured on the samples 7s (a, b, c, d). It doesn't seem to be any remarkable difference on surface energy between the different samples.

The contact angle value is around 78.5°±0.5° on cured epoxy.

3.2 Drop Contact Angle - Carbon fiber plate

The same measurement have been conducted on carbon fiber plates, when they were untreated, after the treatment with atmospheric plasma, on the

same day of the treatment, the day after, the 4th day and the 10th day.

The untreated surface has a contact angle of about 96.5°±0.5°. Attention has been paid on not touching the surface with bare hands, not to affect the measurement.

Treatment has been done on the center of a 1 cm×1 cm area, using a spatially fixed plasma flow, with three combinations of gases: only He, $He + N_2$ and $He + O_2$ (further called HeN_2 and HeO_2). Percentage of $N_2$and O_2has been of about 1%. The length of the plasma flame, between the gun exit and the surface, is about 10 mm.

The duration of exposure to the plasma flow has been 1 and 5 minutes for each combination of gas.

We can see in the graph below the contact angle in function of the days passed from the treatment (day 0 is the treatment day).

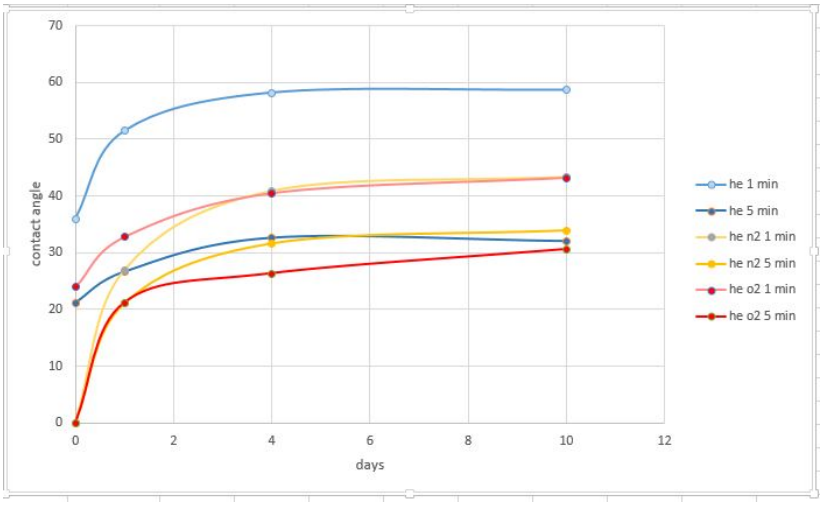

Figure 3.2: Contact angle/days on plate

We can see that the plasma increases significantly the wettability of the surface, reducing the contact angle, especially in the case of HeO_2 for 5 minutes and HeN_2, irrespective of the duration of the treatment. So atmospheric plasma treatment increases the surface energy by incorporating different functional groups.

As one might expect, the longer the treatment, the higher the effect: the value of contact angle stays under 40° even after 10 days in the samples treated for 5 minutes, while the 1 minute treated have the angle between 40° and 60°.

The most important results is that plasma effect lasts enough to have the time of a epoxy resin deposition on a large surface (for instance, a wing crossection): at least for 12 hours, the contact angle remain under 10°.

3.3 Air bubble content

It has been observed that the average value of air bubble diameter in the epoxy is 0,0535±0.00577 mm, but depending on the case, the single sample average air bubble dimension changes, as the number of them, as it can be seen in the following table:

Table 3.1: Average air bubble dimension

sample number	Vacuum (-60 kPa) time (minutes)	Heating temperature (°C)	Heating time (minutes)	Average diameter (mm)
1	none	none	none	0.0497
2	5	none	none	0.0482
3	10	none	none	0.051
4	none	none	none	0.065
5	30	none	none	0.048
6	none	34±1	10	0.051
7	5	34±1	5	0.051
8	10	34±1	10	0.065
9	30	34±1	30	0.055
10	none	none	none	0.048
11	none	40	10	0.057
12	none	40	15	0.052
13	none	40	20	0.055

The average area is 0.1026±0,0321 mm^2 for a cross section of 0.605 mm^2 (700x700 px), that means that 16.97±0.05% is air.

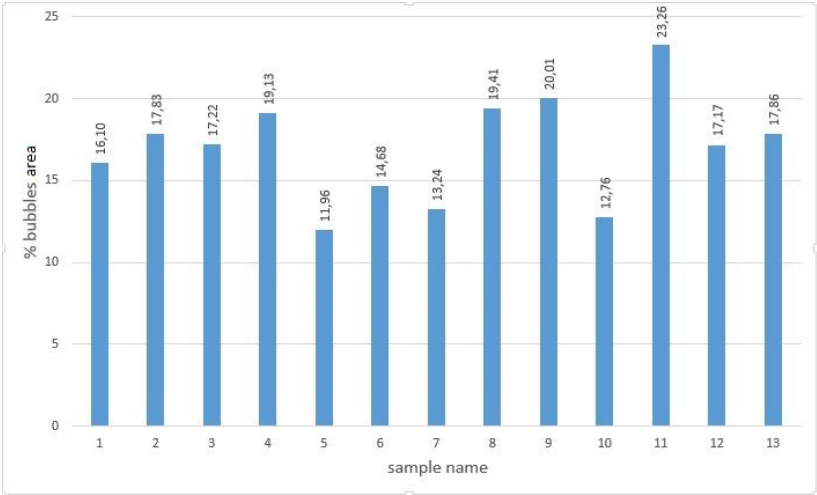

Figure 3.3: % of air

Table 3.2: Bubble statistics

sample number	number of bubbles	total bubble area (mm^2)	% of bubble area
1	44	0.0974	16.09
2	49	0.1079	17.83
3	43	0.1042	17.23
4	23	0.1157	19.13
5	34	0.0723	11.96
6	36	0.0888	14.68
7	33	0.0801	13.24
8	33	0.1576	19.41
9	43	0.1210	20.01
10	33	0.0772	12.76
11	39	0.1407	23.26
12	37	0.1039	17.17
13	37	0.1081	17.86

The variability of the result can be seen from maximum and minimum

value of total area: maximum is for sample 11, minimum for sample 5. This last one has 48.60% less air inside in comparison to sample 11, 25.7% less than the untreated epoxy.

As already mentioned, too much vacuum is bad for the result: increasing the time of vacuum pumping (see samples 7, 8 and 9), the total bubble area increases from 0.0801 to 0.1211, that represents an increase of 51.13%.

The criterion followed for the investigation is the minimum total area of the bubble. The samples 10, 5, 7 and 6 (see graph below) resulted the better ones, so the research focused on them.

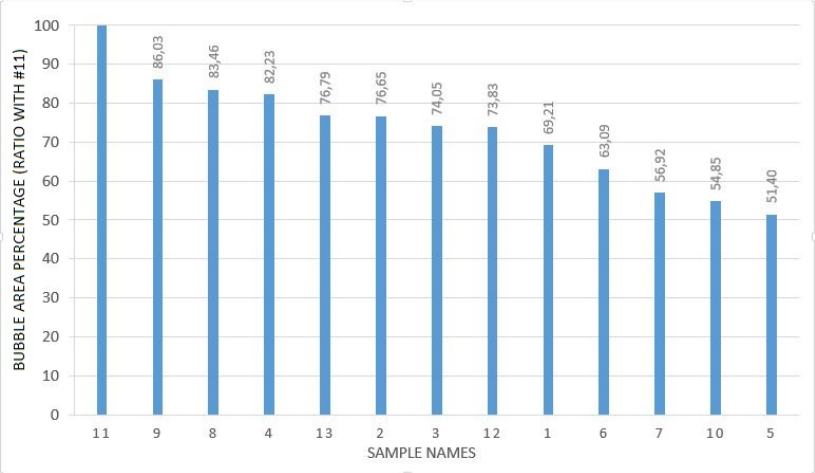

Figure 3.4: Bubble area % in comparison with 11 sample (as 100%)

An air bubble size distribution graph has been obtained from the data:

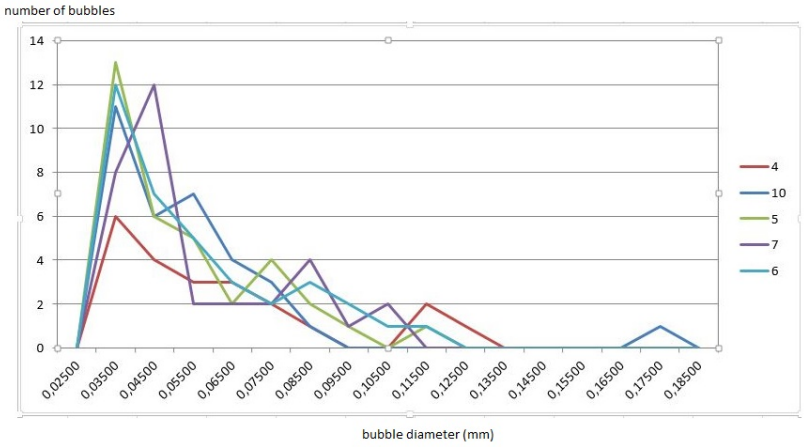

Figure 3.5: Size distribution graph

As we can see, the sample number 4 (no special treatment) has bigger bubbles; this make think that the treatments help big bubbles to degassing from the epoxy

In sample number 6 it's not unusual to find very big bubbles, that can represent a great risk factor for the strength of the linkage.

A more in-depth analysis has been conducted on process number 7, because it avoids the "over bubbling" effect, having only 5 minutes vacuum, and also because, in terms of performance and treatment time, it would be economically worthwhile.

Process 7 analysis For this next step, a faster pump has been used (-60 kPa reached in 1.5 min). Four slightly different experiments have been conducted, to find the best solution. The fixed parameter is pumping time, while temperature has been increased.

The preparation of the crossections was the same of the previous set.

sample	temperature (°C)	vacuum time (min) at -60 kPa	bubbles area (mm^2)
7a	29±1	5	12.99
7b	37±1	5	14.25
7c	45±1	5	14.99
7d	50±1	5	15.01

Table 3.3: Process 7

The curing characteristics are 2 hours at 80° C.

The air bubble content in the cross section is shown below:

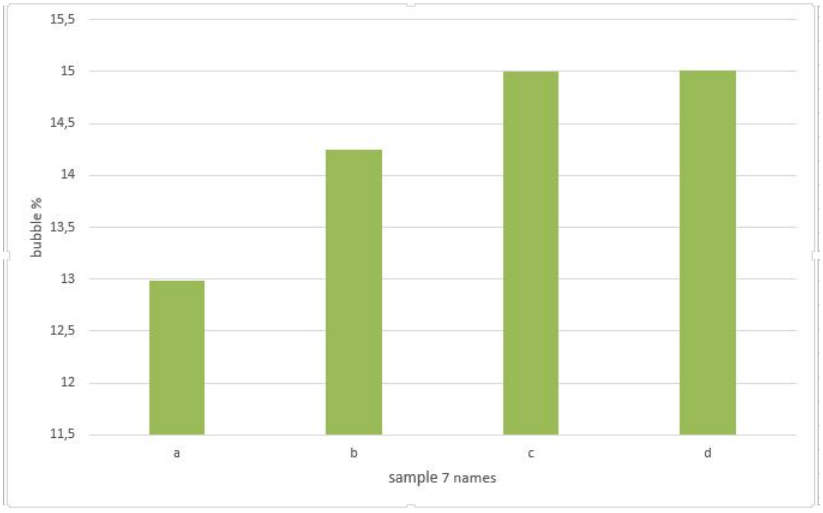

Figure 3.6: Air bubble % in Samples 7s

It seems that increasing the temperature the over bubbling effect is made easier. The difference between 7a sample and 7c/7d samples is about 2% of the total area.

As it concern the dimensions of the bubbles, the bubble diameter average value is shown in the graph below.

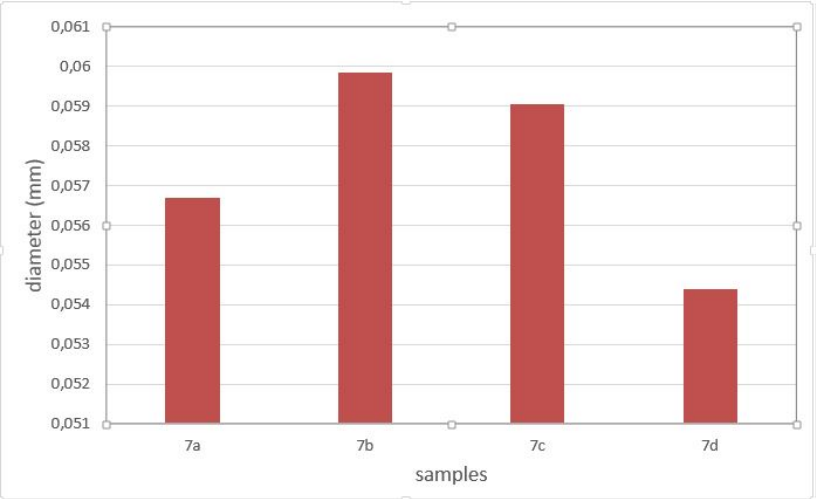

Figure 3.7: bubble diameter average value

It's then preferable to use the first setup and process to limit the bubble air content in the epoxy. This is also favorable in terms of economic aspect, because the energy required is less, as the temperature is lower.

3.4 SEM (scanning electron microscope) - Morphology

These are the images collected during the analysis of the samples: untreated carbon fiber plate, treated with He, $HeN_2$and $HeO_2$for 1 and 5 minutes.

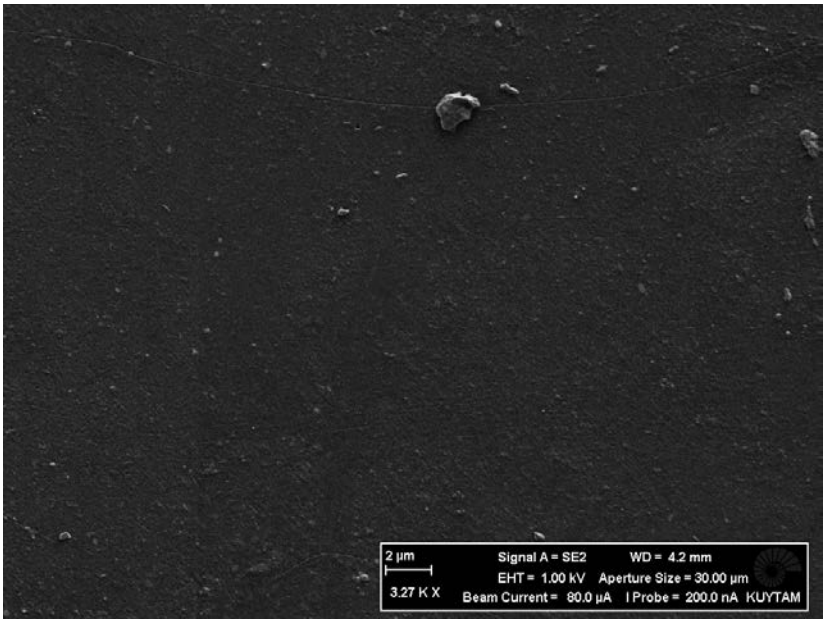

Figure 3.8: Untreated carbon fiber plate

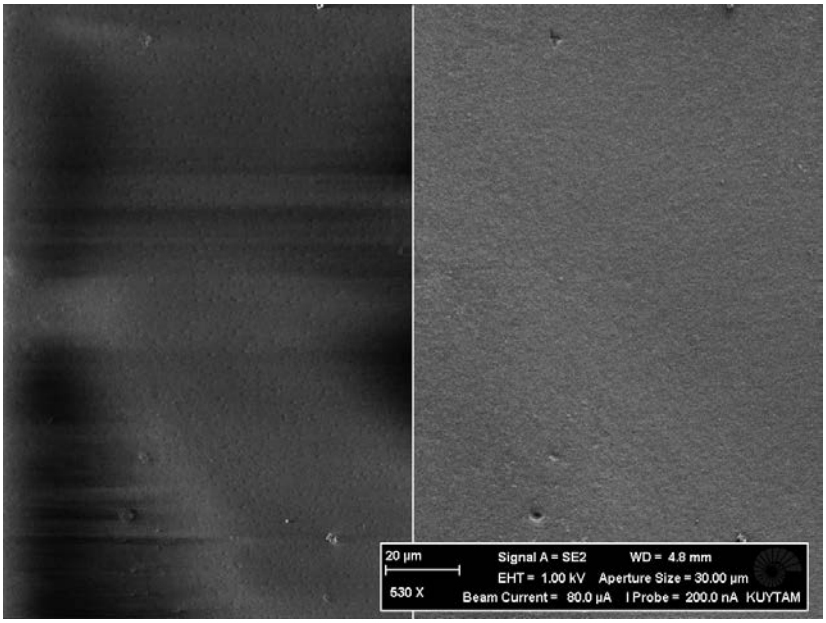

Figure 3.9: Untreated carbon fiber plate

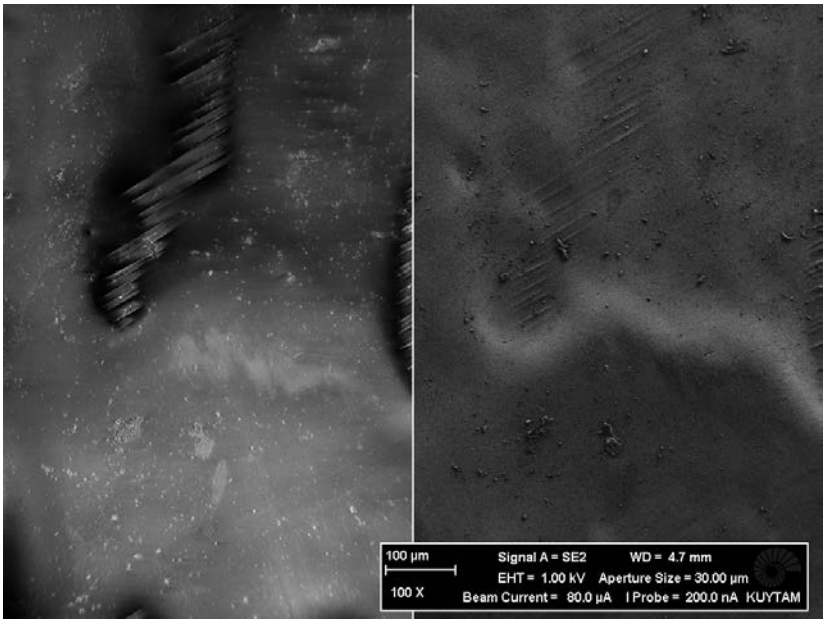

Figure 3.10: Plate treated with He for 1 minute

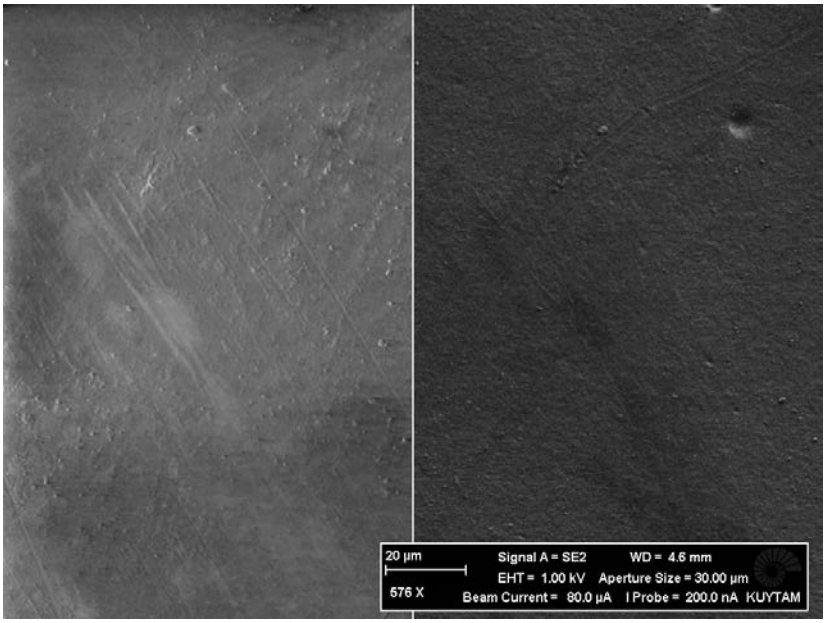

Figure 3.11: Plate treated with He for 1 minute

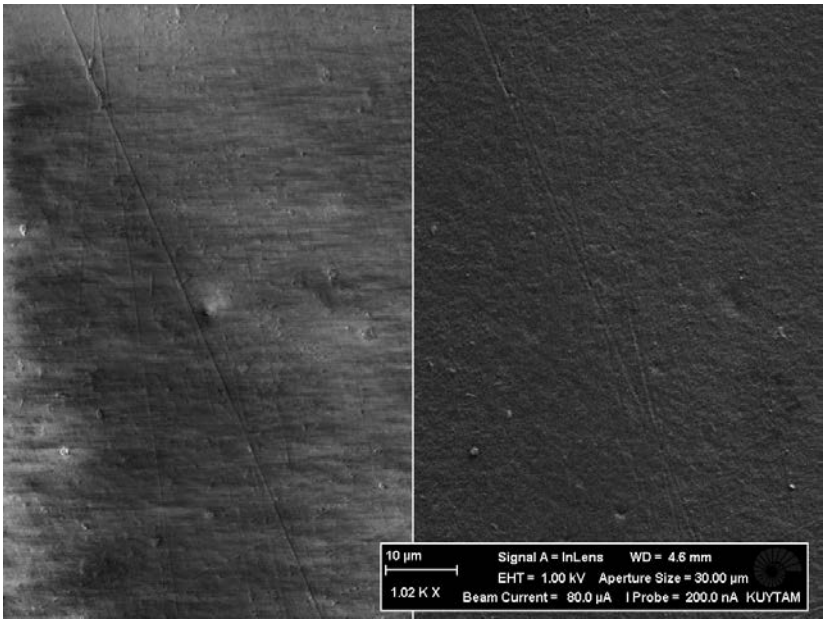

Figure 3.12: Plate treated with He for 5 minute

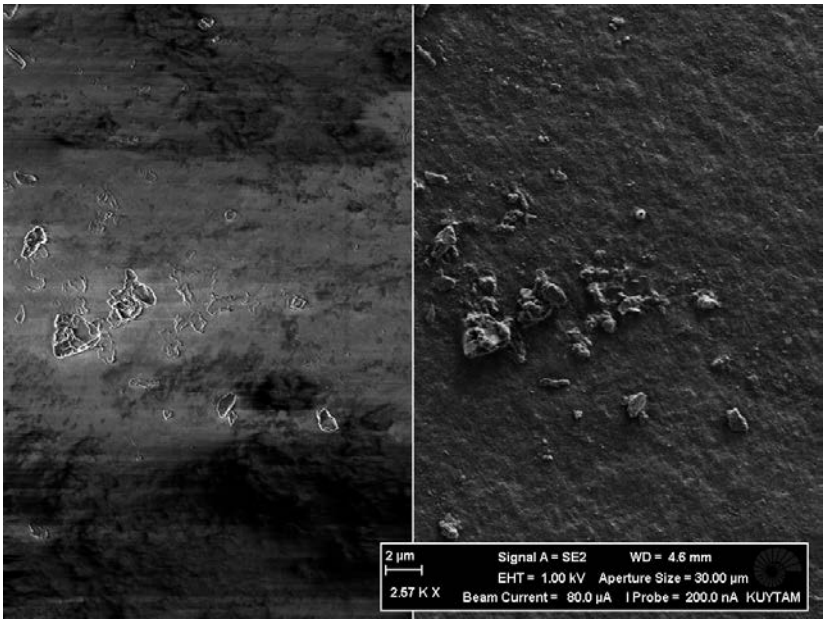

Figure 3.13: Plate treated with HeN_2 for 1 minute

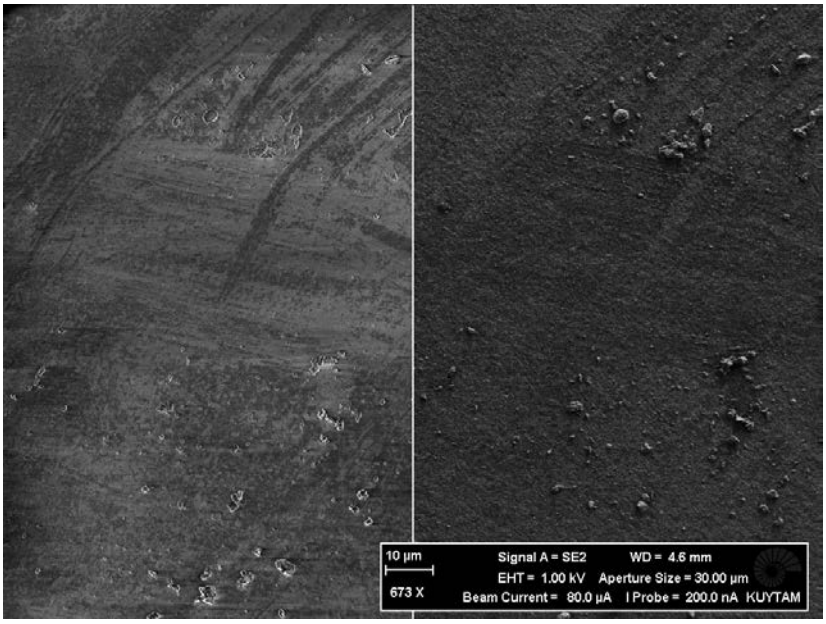

Figure 3.14: Plate treated with HeN_2 for 1 minute

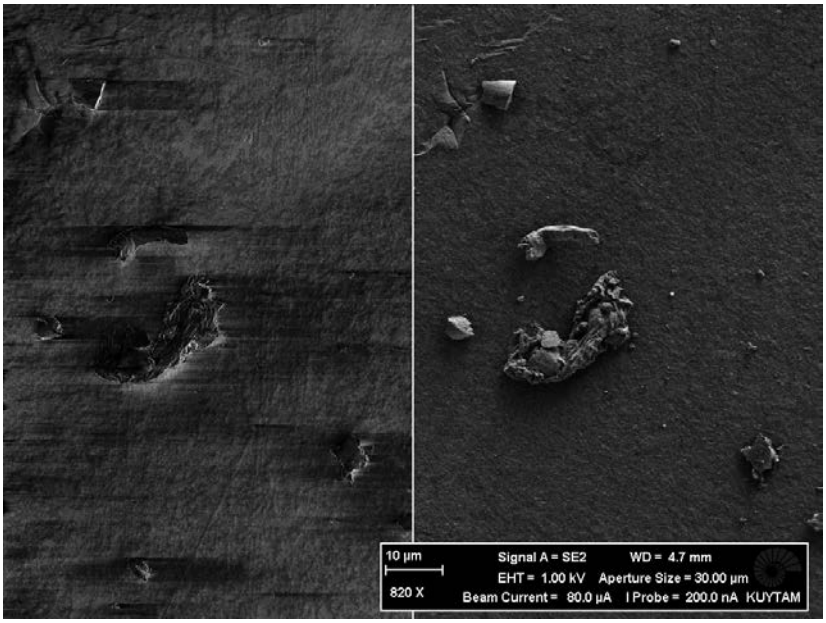

Figure 3.15: Plate treated with HeN_2 for 1 minute

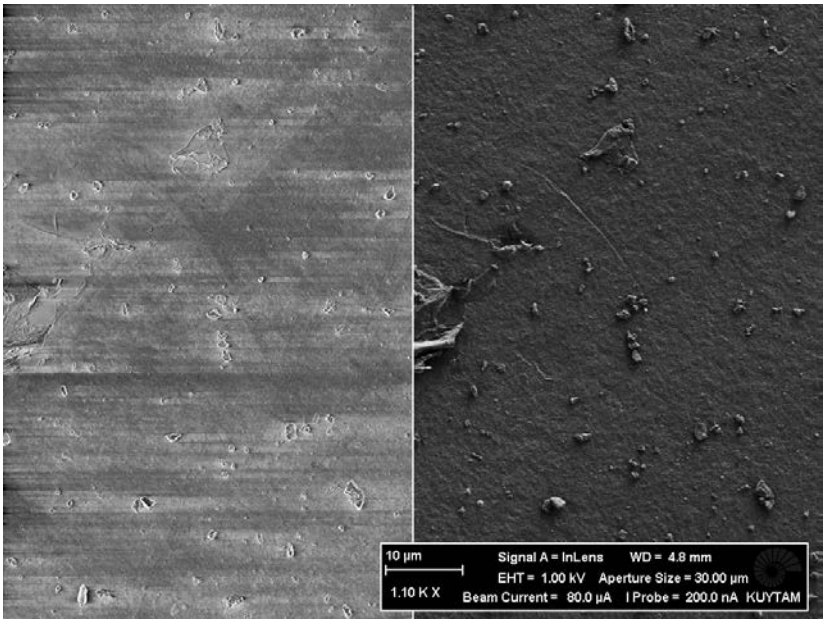

Figure 3.16: Plate treated with HeN_2 for 5 minute

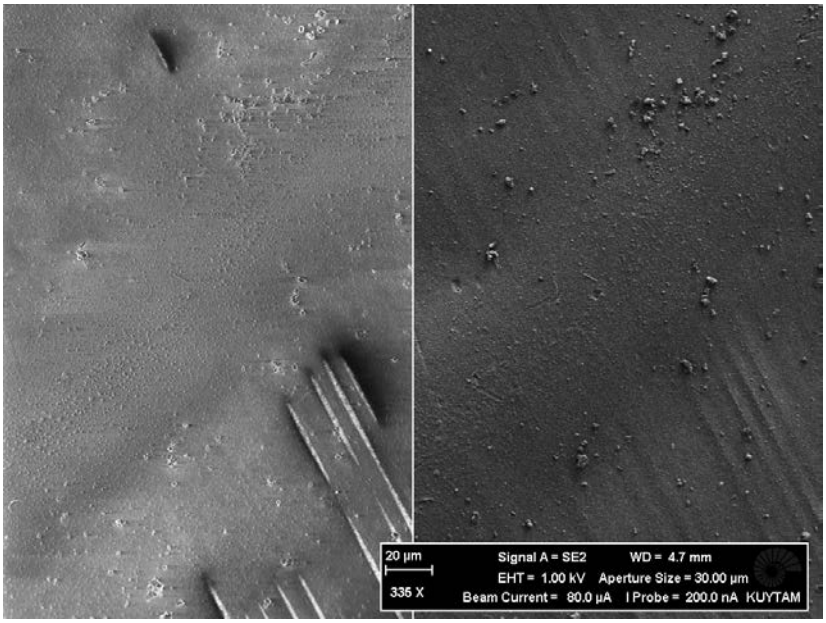

Figure 3.17: Plate treated with HeN_2 for 5 minute

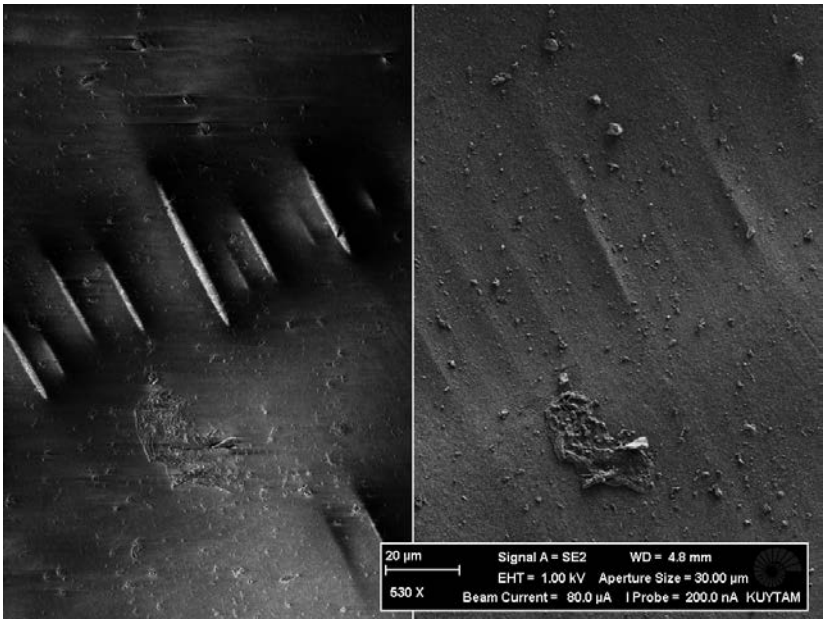

Figure 3.18: Plate treated with HeN_2 for 5 minute

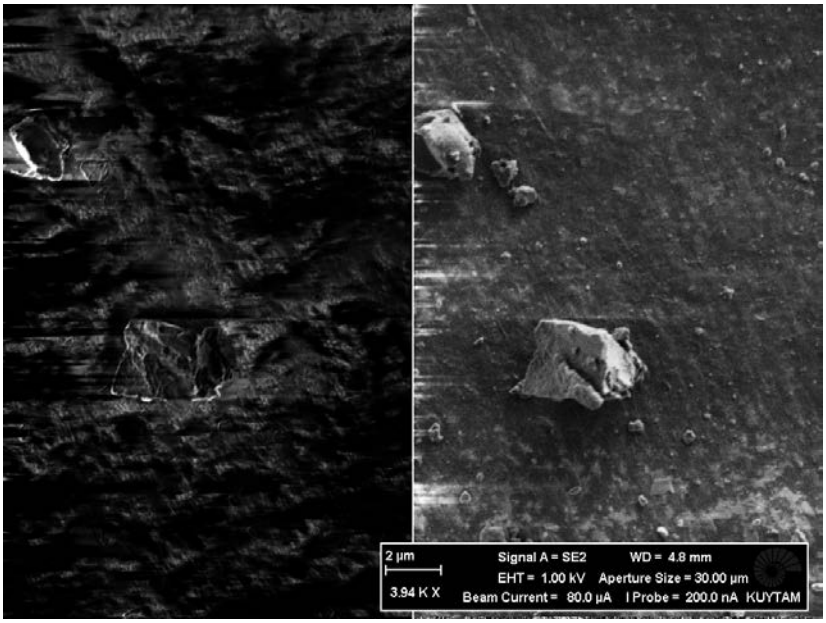

Figure 3.19: Plate treated with HeN_2 for 5 minute

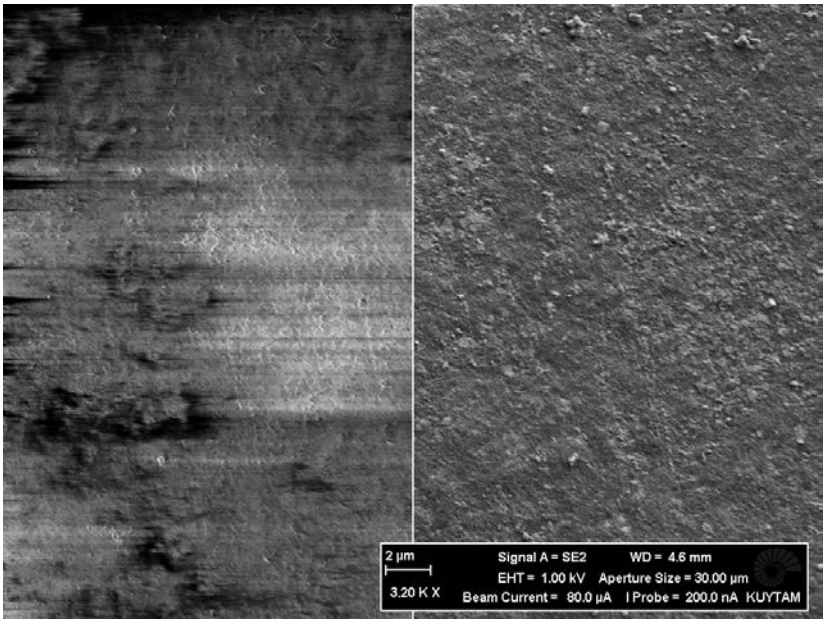

Figure 3.20: Plate treated with HeO_2 for 1 minute

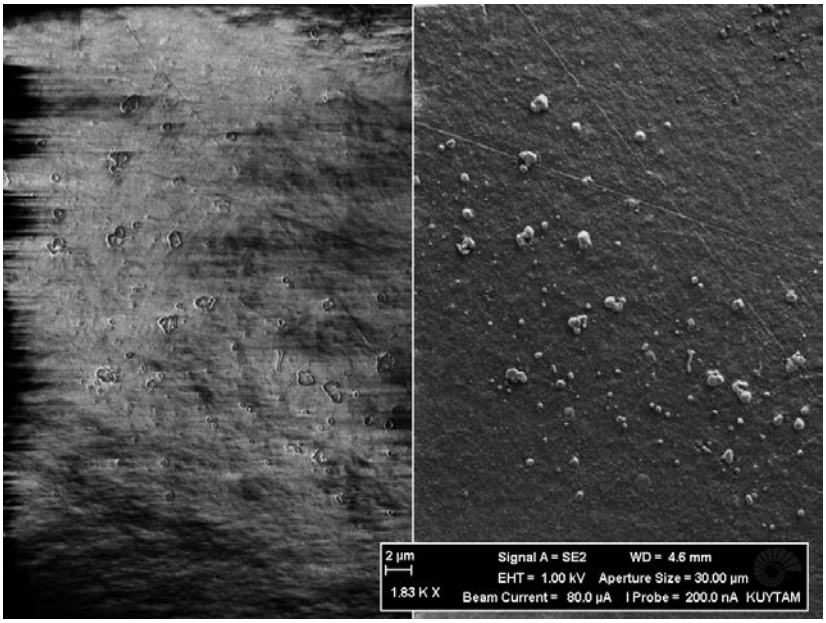

Figure 3.21: Plate treated with HeO_2 for 1 minute

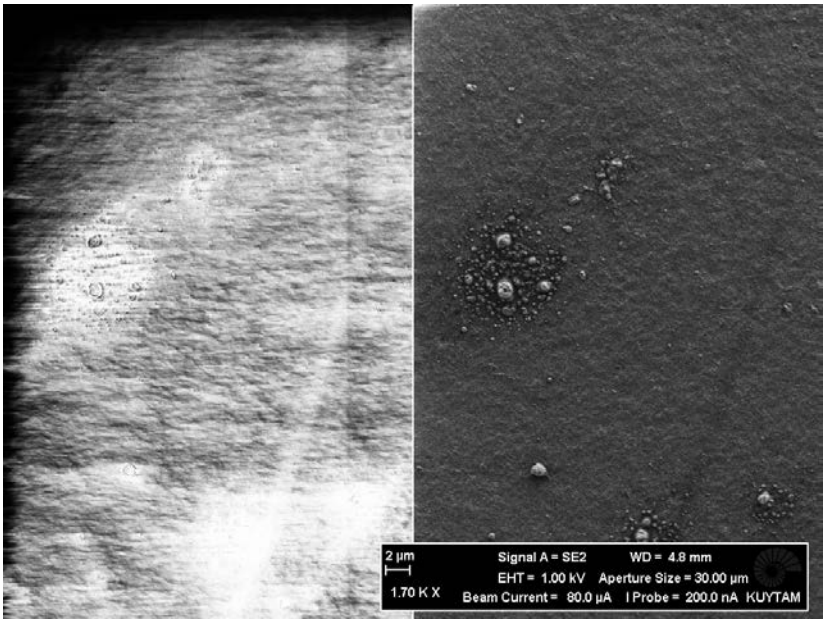

Figure 3.22: Plate treated with HeO_2 for 5 minute

From the images above, a slight increase of the roughness can be observed in some case (e. g. HeN_2 for 1 minute and HeO_2 for 1 minute), but this is not much relevant in terms of increased adhesion of the epoxy resin.

Some particles can be detected, and this can be attributed to some residues of the surface.

The charging effect is evident, and this had obstructed the investigation, so the low voltage beam has been used (EHT = 1.00 kV); this prevented the analysis from going deeper in the magnitude, stopping the accuracy at 2 μm maximum.

We can say then that in this study, no significant roughness has been created nor detected after the atmospheric plasma treatment, unlike Bhowmik and Benedictus research [14].

There is no evidence of damaging of the surface by the plasma beam, so it can be described as gentle towards the surface.

3.5 FTIR

Samples have been analyzed before and right after the treatment, giving the relatives spectra that have been processed with Microsoft Excel™.

The graphs have been then normalized in order to make comparisons between all of them.

The result is shown below:

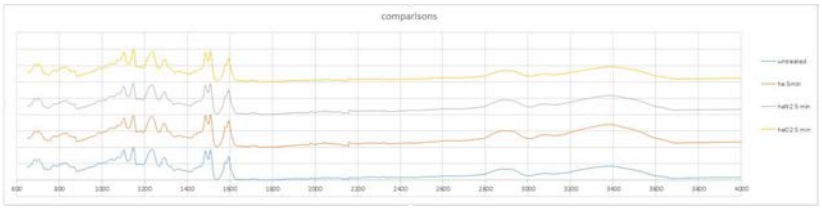

Figure 3.23: FTIR results

As we can see, there are no remarkable differences in the four spectra.

The reason is that FTIR has a penetration in the sample in the order of μm, and the plasma treatment affects only some ηm of the upper surface.

We can say that FTIR is not a suitable technique for this process.

3.6 XPS

Looking at the XPS results, we can better understand how the plasma acts on the surface, which are its interactions and what are the modifications of the surface.

From the Thermo Scientific™ Avantage Data System software the table of composition are obtained. The reported data are the position of the peaks detected (Binding Energy), the FWHM (Full Width at Half Maximum), the area and the percentage of the element selected in the composition of the material. An example of those parameters can be found below:

Name	Peak BE	FWHM eV	Area (P) CPS.eV	Atomic %
C1s Scan A	285.02	1.56	59801.35	36,43
C1s Scan B	286.50	1.50	37871.06	23,09
C1s Scan C	288.34	1.86	8043.87	4,91
C1s Scan D	291.75	2.35	4411.48	2,7
F1s Scan A	688.79	2.18	30637.53	6,18
N1s Scan A	399.74	1.24	7742.81	3,04
N1s Scan B	400.65	1.10	1969.17	0,77
N1s Scan C	400.50	3.37	4566.16	1,79
O1s Scan A	532.71	2.26	81868.58	20,65
Si2p	103.44	0.62	711.19	0,43

Figure 3.24: XPS results table

Observing in particular ratios of Oxygen, Nitrogen, Fluorine and Silica percentages with Carbon percentage, the following remarks can be done:

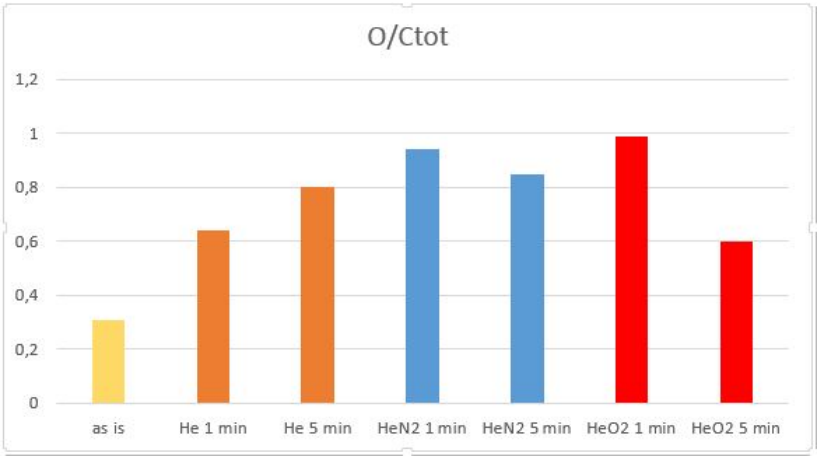

Figure 3.25: O/Ctot

- O/Ctot
  - Compared to the untreated surface (sample "as is"), every process increases the O/C ratio.
  - The ratio with He increases as much as the process is long.
  - With HeO_2 and HeN_2 this is not true: this could be due to etching away the polar groups as plasma duration increases.
  - With shorter exposure time, HeO_2 and HeN_2 obtain a higher O/C ratio than He
  - The maximum O/C ratio is with HeO_2 1 min.

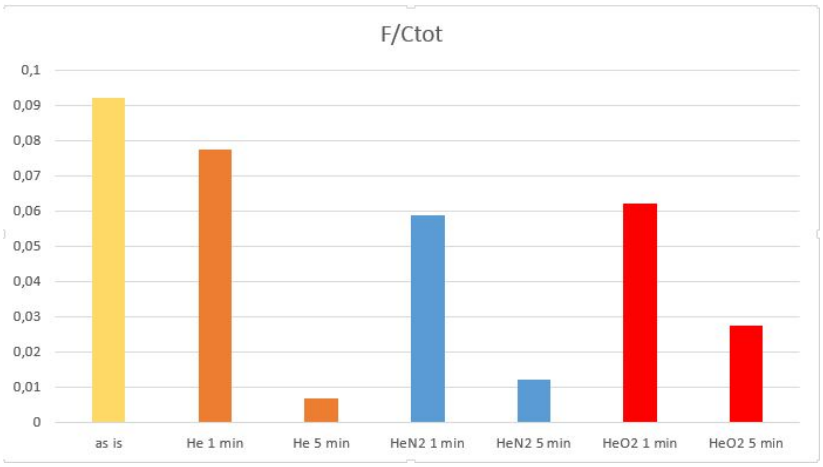

Figure 3.26: F/Ctot

- F/Ctot
  - The plasma treatment with the three gases decreases the F/C ratio as much as the treatment is long.
  - The best process to minimize F/C is He 5 min.

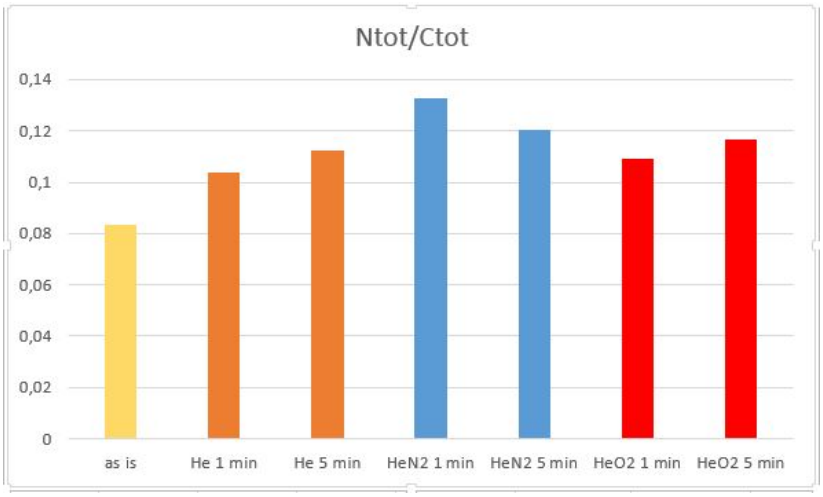

Figure 3.27: N/Ctot

- N/Ctot
  - The increase is proportional with time (not for HeN_2).
  - The highest increase is obtained with HeN_2 for 1 minute.

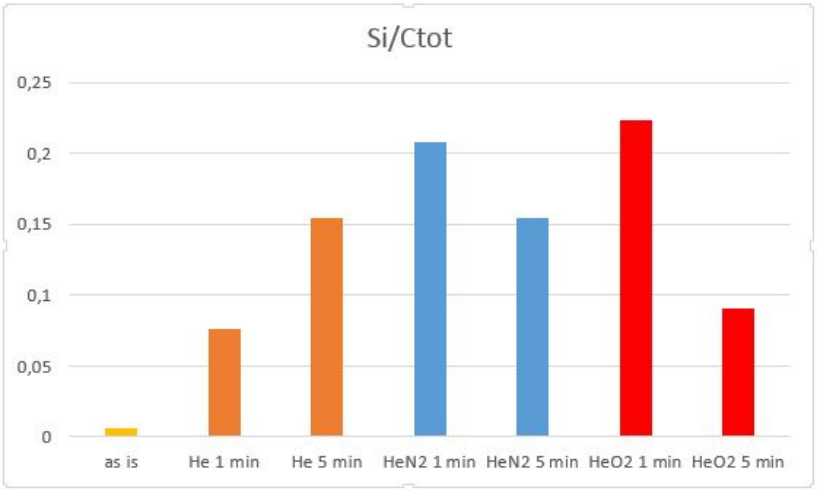

Figure 3.28: Si/Ctot

- Si/Ctot
  - The increase is proportional with time with He. This is maybe because Si is subsurface, and, due to the etching of the surface, comes up after a while.
  - With HeO_2 and HeN_2 this is not true.

Another scanning has been conducted, generating a map in a square area of 15mm×15mm, with more than 700 points of XPS analysis. The mapping shows the presence of the different chemical groups on the surface. As it can be seen, several chemical groups are detected on the surface after the plasma treatment. These are: $-CH_2-$, $C-NH_2$, $-NO_2$, $-COOH$, $-CF_2$. 4 species of C, 2 of O, N and F are detected. Looking to the similar shapes on the mapping it has been possible to identifie the molecular groups of each species, as shown in the images below.

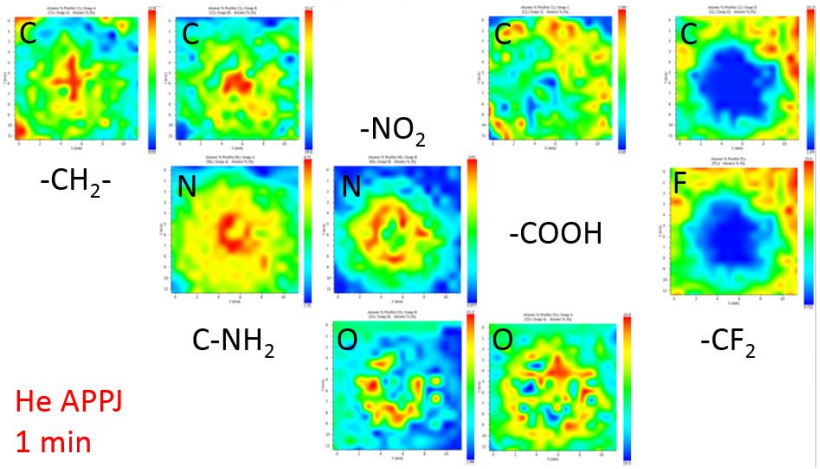

Figure 3.29: Mapping of He 1 min

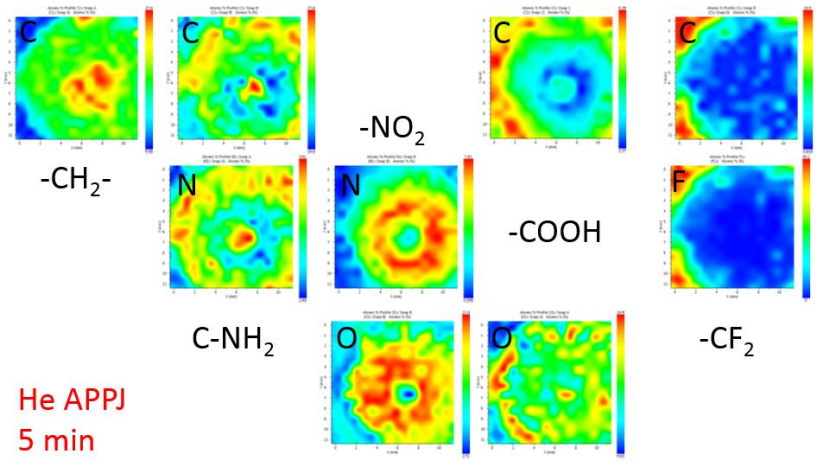

Figure 3.30: Mapping of He 5 min

Those results show that APP treatment with Helium,$-NH_2$ functional groups are activated on the surface in the shape of a ring, as the time of the treatment increases. After 5 minutes, the presence of these groups decreases at the center of the area, where the plasma beam hit the surface.

$-CF_2$ groups are eliminated by the treatment, more efficiently with the increase of the time.

The other groups open up from the center of the area as the time of treatment is increased.

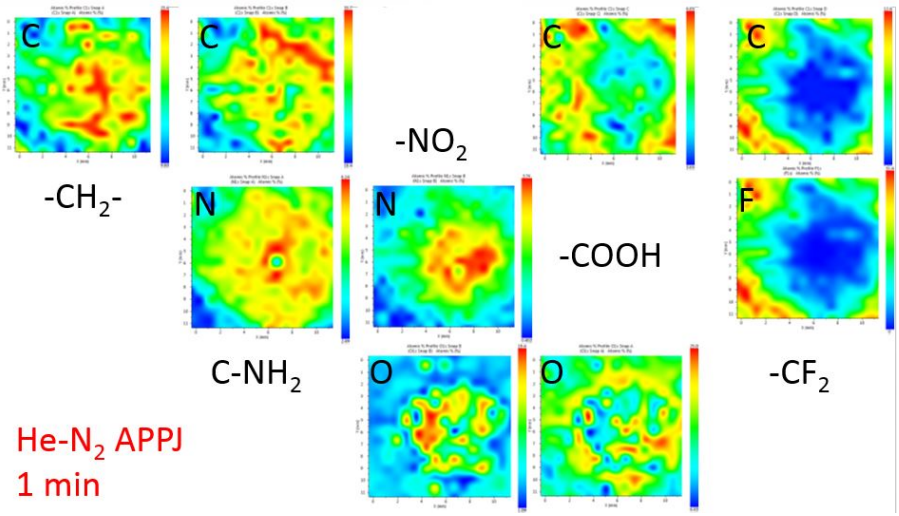

Figure 3.31: Mapping of HeN_2 1 min

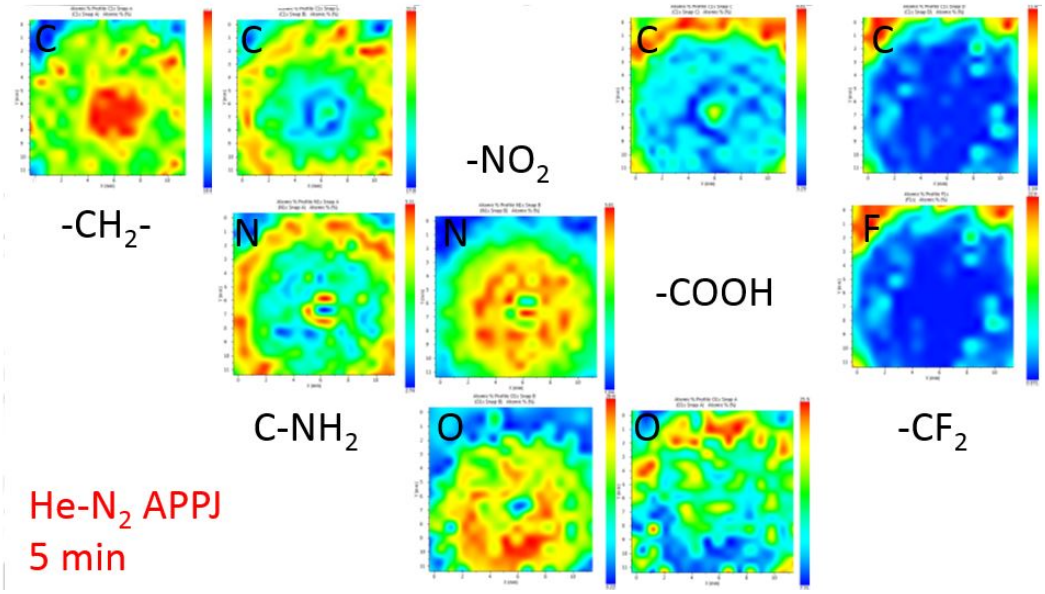

Figure 3.32: Mapping of HeN_2 5 min

Those results show that APP treatment with HeN_2,$-NH_2$ functional groups are activated on the surface in the shape of a ring, as the time of the treatment increases. It can be observed that already after 1 minute, the presence of these groups starts decreasing at the center of the area, where the plasma beam hit the surface (small blue area). This can signify that HeN_2 treatment is more effective than the treatment with simply He.

The concentration of $-NO_2$ is significant, especially after 5 minutes, because it's widespread on the sample, quite without signs of decreasing in the center of the plasma treated area.

$-CF_2$ groups are eliminated by the treatment, more efficiently with the increase of the time.

The other groups open up from the center of the area as the time of

treatment is increased, increasing their concentration.

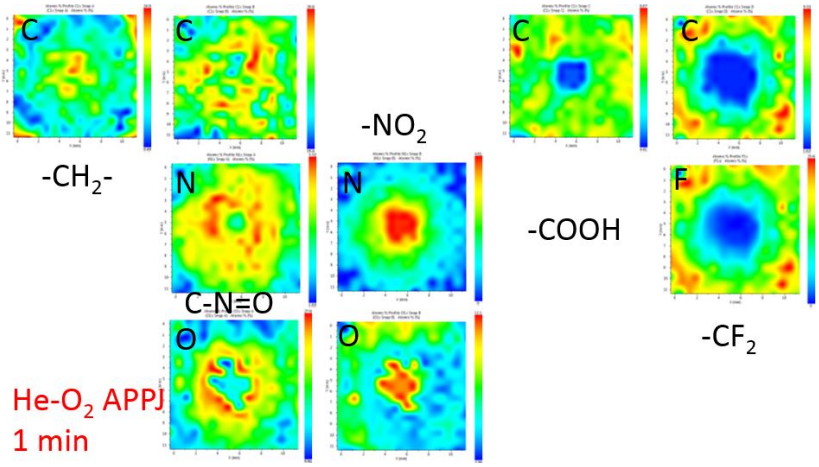

Figure 3.33: Mapping of $HeO_2$1 min

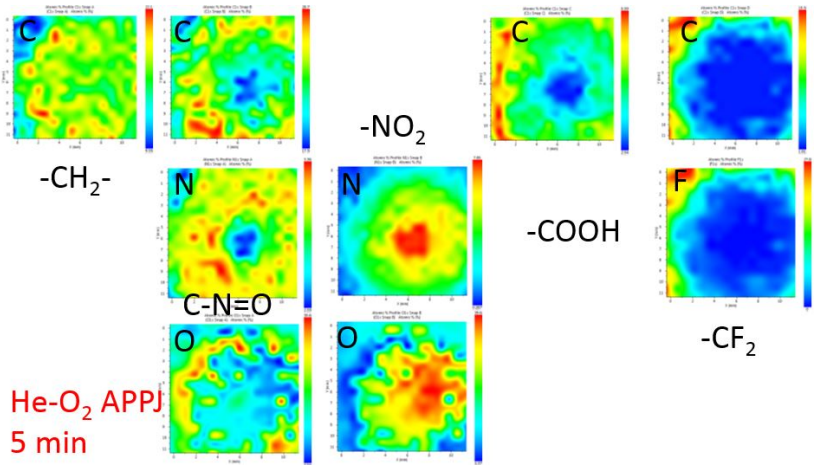

Figure 3.34: Mapping of HeO_2 5 min

Those results show that APP treatment with HeO_2, $-NO_2$ functional groups are activated on the center of the surface, as much as the time of the treatment is long. After 5 minutes, the presence of these groups is less then

with the other two gases, but it doesn't show the ring shape that could be counter-productive for the adhesion. This aspect can be attributed to the O atoms supplied by the plasma.

$-CF_2$ groups are eliminated by the treatment as well as the other treatments, more efficiently with the increase of the time.

The other groups open up from the center of the area as the time of treatment is increased, and are pushed at the external part of the square surface.

3.7 Shear test

First scan results Shown below, there are the results of the first samples, treated with the first scan method.

The samples' names refer to the different plasma treatments:

- sample #1: Helium
- sample #2: Helium + Nitrogen
- sample #3: Helium + Oxygen

Table 3.4: First scan shear test results

	Max.Load (kN)	Width (mm)	Bond Length (mm)	Shear Strength (MPa)
1	6.08	25.00	28.96	8.4
2	9.72	24.79	35.41	11.1
3	5.05	24.92	31.49	6.4
Mean	6.95	24.90	31.95	8.6
S.D.	2.45	0.11	3.25	2.3
Minimum	5.05	24.79	28.96	6.4
Maximum	9.72	25.00	35.41	11.1

We can see in the last column that the shear strength ($= \frac{Max.Load}{Width*BondLenght}$) for sample #2 is about 11.1 MPa. This is a good result, since the best result obtained for untreated surfaces, with the same epoxy glue, is 8.5 MPa, that means that this research succeeded in an increase of 30.5% in the strength.

The good strength result is encouraging, but there is a but, however: the failure is adhesive and not, as desired at least, cohesive (see picture below). This means that the epoxy-substrate interface is not enough strong yet.

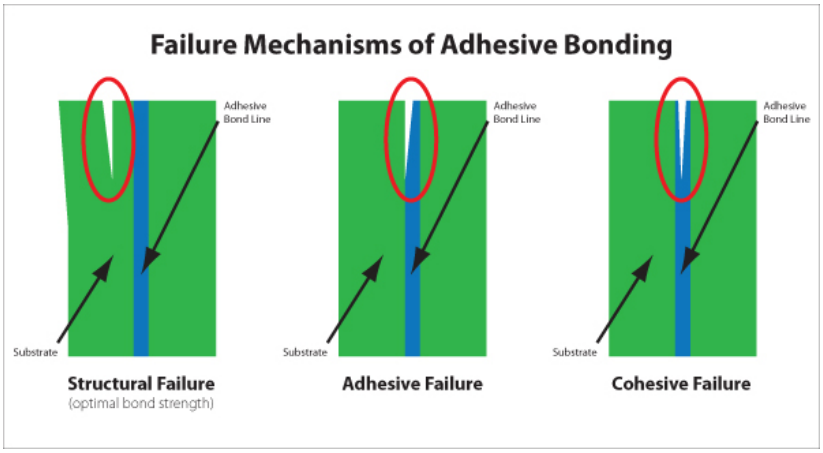

Figure 3.35: Failure mechanisms of adhesive bonding

To be thorough, here there is the load-displacement graph for the three samples:

Table 3.5: Second scan shear test results

samples names	Max. Load (kN)	Shear Strength (MPa)
1	5.22	8.35
2	7.63	12.21
3	5.50	8.80
4	4.13	6.61
5	7.13	11.41
6	6.16	9.86

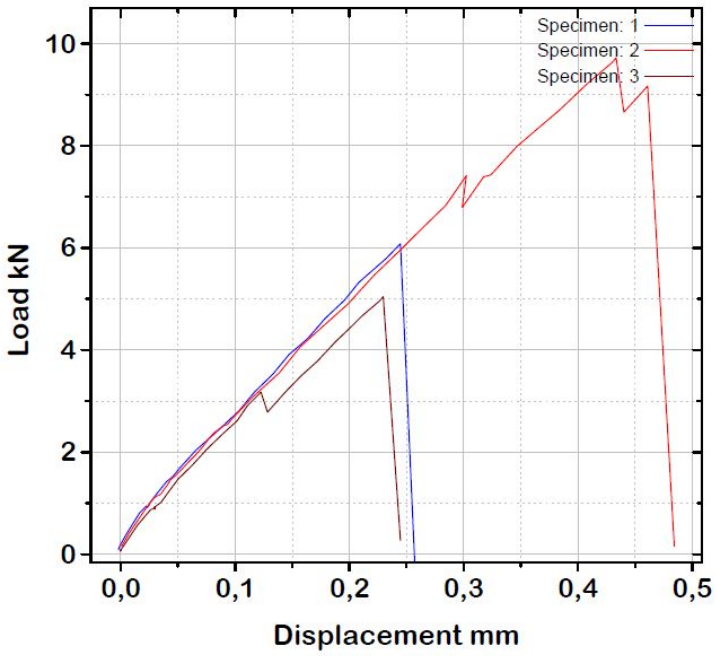

Figure 3.36: Load-displacement graph: 1st scan

Second scan results In this second scan, samples have been treated with two different plasmas: samples #1-3 are treated with the 6 kHz plasma device, while samples #4-6 with the RF (Radio Frequency) plasma device. The epoxy used during this test campaign has been the Hysol© EA9394.

The lap-shear strength in megapascals (MPa) of the bonded joints was defined as the peak load divided by the overlap area (standard to $25 \times 25\ mm^2$). As we can see, in this case too He/N_2treatment seems to be more efficient, reaching a maximum shear strength of 12.21 MPa. There are no relevant differences in results between the two different plasma devices treatments.

To be thorough, here there is the load-displacement graph for the three samples:

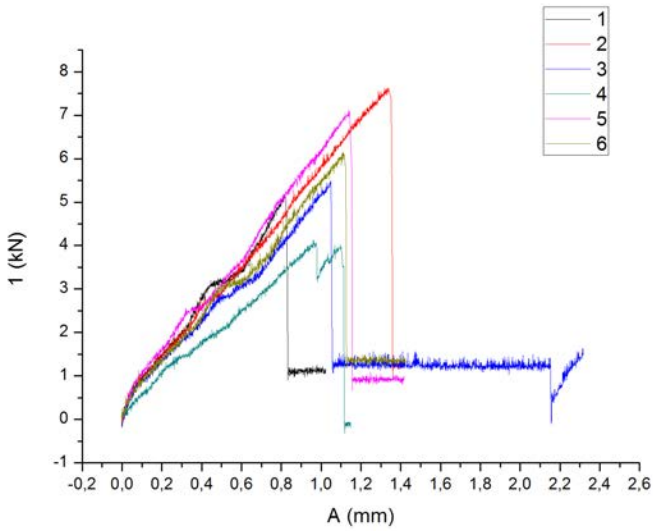

Figure 3.37: Load-displacement graph: 2nd scan

The bigger displacement, compared to the one of the first lap-shear test, is probably due to the different epoxy resin used in the second time. It is about 3 times bigger.

4 Conclusions

The influence of atmospheric plasma on surfaces of carbon fibers composites had been studied.

The degree of surface activation depends on the treatment duration. The maximum period of treatment studied is 5 minutes. XPS confirms that chemical groups were successful introduced using atmospheric plasma treatment. The highest degree of $-NO_2$ groups, that are the one responsible to adhesion of the epoxy resin, are obtained with He/N_2 and He treatments. Fluorinate groups are equally erased by the three gases, no important differences are observed. It's remarcable that 5 minutes can be too long for the adhesion of chemical groups, in terms that, after the deposition of these ones an erosion can occur by the plasma beam. We can see that He/N_2 is the most effective miture of gases that increases N content on the surface, in 1 minute it gives even more percentage than the other gases in 5 minutes. Furthermore, the mapping obtained with XPS shows how better is the He/N_2 treatment in terms of homogeneous coverage of the samples.

The atmospheric plasma doesn't cause significant damage to the surfaces, as it can be observed with SEM analysis. This signify that the plasma generated in the lab is not aggressive towards the surface. However, and this is a negative aspect, not even a change in roughness is notified, characteristic that could help adhesion of epoxy.

FTIR investigation doesn't lead to relevant results: this technique has a penetration in the sample in the order of μm, and the plasma treatment

affects only some ηm of the upper surface. We can say that FTIR is not a suitable technique for this process.

The results from contact angle measurements show that the hydrophobicity of carbon fibers decreased significantly (still half of the value of the untreated surface even after 10 days -with stable value at 45°-). Once again, He/N_2 seems to be the most effective treatment, decreasing the contact angle to 0° after 1 minute of treatment.

For what it concerns the air bubbles in the epoxy layer, it has been shown that the air content is not negligible, reaching in some case 23.3% of the cross section area. Various method have been tried.

The process that limit the air bubble presence is the one that consider using vacuum coupled with the heating of the epoxy resin substrate.

The optimal parameters that seems to work properly with Hysol© epoxies are found to be:

- vacuum: -60kPa, held for 5 min
- heating temperature of the plate: 29±1°C, held for the duration of vacuum process

The amount of air is decreased from 16% to 12% of the total area, that means a decrease of 25.7%, with an average bubble diameter of about 0.0565 mm.The process duration is short (5 min), and this is a good economic aspect, in addition to limiting the over bubbling effect that occurs when the vacuum is held for a longer period of time.

According to the lap-shear strength tests of the bonded joints, the best treatment seems to be He/N_2, as it is the most efficient, reaching a maximum shear strength of 12.21 MPa, which represents an increase of 43% of the strength without treatments. There are no relevant differences in results between the two different plasma devices (6kHz and Radio Frequency) treatments.

In conclusion, atmospheric plasma with He and 1% N_2 is a useful technique to provide better adhesion properties to the surface of carbon fiber composites reinforced with phenolic resin matrix. In addition to this, atmospheric plasma is characterized by its high environmental efficiency and easy implementation at industrial level.

Acknowledgments

I am grateful to Professor Özgür Birer of Koç University, Istanbul. I am extremly thankful and indebted to him for sharing expertise, and sincere and valuable guidance and encouragement extended to me, also for providing me with all the necessary facilities for the research.

I wish to express my sicere thanks to Giovanni Lucchetta, my lecturer, for the good relationship we built during this important path for me.

I also thank my parents and my sister for the unceasing encouragement, support and attention.

Bibliography

[1] Bowditch MR, Shaw SJ. Adhesive bonding for high performance materials. Adv Perform Mater 1996;3:325–42.

[2] Shenton MJ, Lovell-Hoare MC, Stevens GC. Adhesion enhancement of polymer surfaces by atmospheric plasma treatment. J Phys D: Appl Phys 2001;34: 2754–60.

[3] Uren˜a A, Gude RM, Prolongo SG. Carbon nanofibers reinforced adhesives for joining carbon fiber epoxy composites. 13th European conference on composite materials, 2008.

[4] Custo´ dio J, Broughton J, Cruz H. A review of factors influencing the durability of structural bonded timber joints. Int J Adhes Adhes 2009;29: 173–85.

[5] Bhowmik S, Bonin HW, Bui VT, Weir RD. Modification of high-performance polymer composite through high-energy radiation and low-pressure plasma for aerospace and space applications. J Appl Polym Sci 2006;102:1959–67.

[6] Chan C-M, Ko T-M. Polymer surface modification by plasmas and photons. Surf Sci Rep 1996;24:1–54.

[7] Noeske M, Degenhardt J, Strudthoff S, Lommatzsch U. Plasma jet treatment of five polymers at atmospheric pressure: surface modifications and the relevance for adhesion. Int J Adhes Adhes 2004;24:171–7.

[8] Y. Qiu, N. Anantharamaiah, S. Xie, N.P. Vaidya, C. Zhang, Adv. Compos. Lett. 10 (2001) 135.

[9] Y. Qiu, Y.J. Hwang, C. Zhang, B.L. Bures, M. McCord, J. Adhes. Sci.

Technol. 16 (2002) 449.

[10] Y. Qiu, C. Zhang, Y.J. Hwang, B.L. Bures, M. McCord, J. Adhes. Sci. Technol. 16 (2002) 99.

[11] Rotheiser J. Joining of plastics: handbook for designers and engineers. Munich: Hanser; 1999.

[12] Roth JR. Industrial plasma engineering. Bristol, Philadelphia: The institute of physics publishing; 2000.

[13] Edward PM. Adhesives and sealants. New York: McGraw-Hill; 2007.

[14] S.Bhowmik, R.Benedictus Surface modification of high performance polymers by atmospheric pressure plasma and failure mechanism of adhesive bonded joints. Int J Adhes Adhes 2010; 4:418–24.

[15] C. Tendero, C. Tixier, P. Tristant, J. Desmaison, P. Leprince Atmospheric pressure plasmas: A review. Spectrochimica Acta Part B 61 (2006) 2 – 30

[16] A.F. Stalder, G. Kulik, D. Sage, L. Barbieri, P. Hoffmann. A Snake-Based Approach to Accurate Determination of Both Contact Points and Contact Angles.

Colloids And Surfaces A: Physicochemical And Engineering Aspects, vol. 286, no. 1-3, pp. 92-103, September 2006.

[17] A.F. Stalder, T. Melchior, M. Müller, D. Sage, T. Blu, M. Unser Low-Bond Axisymmetric Drop Shape Analysis for Surface Tension and Contact Angle Measurements of Sessile Drops. Colloids and Surfaces A: Physicochemical and Engineering Aspects, vol. 364, no. 1-3, pp. 72-81, July 20, 2010.

[18] R. P. Woodward Contact Angle Measurements Using the Drop Shape Method. , Ph.D Thesis, First Ten Angstroms, Portsmouth.

[19] Y. Ren, C. Wang, Y. Qiu. Aging of surface properties of ultra high modulus polyethylene fibers treated with He/O2 atmospheric pressure plasma jet. Surface & Coatings Technology 202 (2008) 2670–2676

[20] Hysol EA 9380 Henkel Corporation Aerospace Group Guide

[21] M. Green, F. Guild, R. Adams. Int J Adhes Adhes 2002;22:81.

[22] H. Herrmann, G. Selwin, J. Park, I. Henins, L. Rosocha. Atmospheric pressure plasma jet. Los Alamos national laboratory, P-24 Plasma Physics, M/S E526, Los Alamos,NM87544, USA

[23] H.M.S. Iqbal,S.Bhowmik n, R.Benedictus. Surface modification of high performance polymers by atmospheric pressure plasma and failure mechanism of adhesive bonded joints. Int J Adhes Adhes 30(2010)418–424

[24] Zaldivar RJ, Nokes J, Steckel GL, Kim HI, Morgan BA. The Effect of Atmospheric plasma treatment on the chemistry, morphology and resultant bonding behavior of a pan-based carbon fiber-reinforced epoxy composite. J Compos Mater 2010;44(2):137–56.

[25] Zaldivar RJ, Salfity J, Steckel G, Morgan B, Patel D, Nokes JP, Metal Bondability of TC410 composites: the surface analysis and wetting properties of an atmospheric plasma-treatedsiloxane-modified cyanate ester composite. J Compos Mater 2011;46(16):1925–36.

[26] Pulpytel J, Kumar V, Peng P, Micheli V, Laidani N, Arefi-Khonsari F. Deposition of organo silicon coatings by a non-equilibrium atmospheric pressure plasma jet: design, analysis and macroscopic scaling law of the process.

Plasma Process Polym2011;8(7):664–75.

[27] Lommatzsch U, Pasedag D, Baalmann A, Ellinghorst G, Wagner Hans-Erich. Atmospheric pressure plasma jet treatment of polyethylene surfaces for adhesion improvement. Plasma Process Polym 2007;4:S1041–5.

[28] Bismarck A, BrostowW, Chiu R, Hagg Lobland HE, Ho KKC. Effects of surface plasma treatment on tribology of thermoplastic polymers. Polym Eng Sci 2008:1971–6.

[29] Baltazar Y., Jimenez A, Bistritz M, Schulz E, Bismarck A. Atmospheric air pressure plasma treatment of lignocellulosic fibres: impact on mechanical properties and adhesion to cellulose acetatebutyrate. ComposSciTechnol 2008;68:215–27.

[30]Quintiere JG, Walters RN, Crowley S. Flammability properties of aircraft carbon-fiber structural composite. Finalreport.U.S.Department of Transportation Federal Aviation Administration. DOT/FAA/AR-07/57;2007.

[31] H. Schonhorn, R. Hansen, J. Appl. Polym. Sci. 11 (1967) 1461.

[32] H. Conrads, M. Schmidt, Plasma generation and plasma sources, Plasma Sources Sci. Technol. 9 (2000) 441–454.

[33] C Tendero, C. Tixier, P. Tristant, J. Desmaison, P. Leprince. Atmospheric pressure plasmas: A review. Spectrochimica Acta Part B 61 (2006) 2 – 30

[34] N.S.J. Braithwaite, Introduction to gas discharges, Plasma Sources Sci. Technol. 9 (2000) 517– 527.

[35] H.R. Griem, High-density corrections in plasma spectroscopy, Phys. Rev. 128 (3) (1962) 997– 1003.

[36] M. Moisan, M.D. Calzada, A. Gamero, A. Sola, Experimental investigation and characterization of the departure from local thermodynamic equilibrium along a surface-wave-sustained discharge at atmospheric pressure, J. Appl. Phys. 80 (1) (1996) 46– 55.

[37] M.I. Boulos, P. Fauchais, E. Pfender, Thermal Plasmas: Fundamental And Applications. Volume I, Plenum Press, New York, ISBN: 0-306- 44607-3, 1994, 452 pp.

[38] H.R. Griem, Validity of local thermal equilibrium in plasma spectroscopy, Phys. Rev. 131 (3) (1963) 1170–1176.

[39] M.D. Calzada, A. Rodero, A. Sola, A. Gamero, Excitation kinetic in an argon plasma column produced by a surface wave at atmospheric pressure, J. Phys. Soc. Jpn. 65 (4) (1996) 948– 954.

[40] R.H. Huddlestone, S.L. Leonard, Plasma Diagnostic Techniques, Academic Press, New York, 1965.

[41] H.R. Griem, Plasma Spectroscopy, McGraw-Hill, New York, 1964.

[42] W. Lochte-Holtgreven, Plasma Diagnostics, North-Holland, Amsterdam, 1968.

[43] M. Mitchner, C.H. Kruger Jr., Partially Ionized Gases, Wiley, New York, 1973.

[44] Y.Choia, J. Kima, K. Paekb, W. Jub, Y.S. Hwanga. Characteristics of atmospheric pressure N2 cold plasma torch using 60-Hz AC power and its application to polymer surface modification. Surface & Coatings Technology 193 (2005) 319– 324

[45] J. Abenojar, M.A. Martìnez, N. Encinas, F. Velasco. Modification of

glass surfaces adhesion properties by atmospheric pressure plasma torch. International Journal of Adhesion & Adhesives 44(2013)1–8

[46] V. Law, J. Mohan, F. T. O'Neill, A. Ivankovic, D. P. Dowling. Air based atmospheric pressure plasma jet removal of FreKote 710-NC prior to composite-to-composite adhesive bonding. International Journal of Adhesion&Adhesives 54 (2014) 72–81

[47] M. Noeske, J. Degenhardt, S. Strudthoff, U. Lommatzsch. Plasma jet treatment of five polymers at atmospheric pressure: surface modifications and the relevance for adhesion. Int J of Adhes Adhes 24 (2004) 171–177

[48] V. Fombuena, J. Balart, T. Boronat, L. Sánchez-Nácher, D. Garcia-Sanoguera. Improving mechanical performance of thermoplastic adhesion joints by atmospheric plasma. Materials and Design 47 (2013) 49–56

[49] P. Calvo O, L. Sanchez-Nacher, MA. Bonet, D. Garcia-Sanoguera, R. Balart. Optimization of adhesive joints of low density polyethylene (LDPE) composite laminates with polyolefin foam using corona discharge plasma. J Appl Polym Sci 2009;114:2971–7.

[50] De Geyter N, Morent R, Leys C. Surface characterization of plasma-modified polyethylene by contact angle experiments and ATR-FTIR spectroscopy. Surf Interface Anal 2008;40:608–11

[51] Thurston RM, Clay JD, Schulte MD. Effect of atmospheric plasma treatment on polymer surface energy and adhesion. J Plast Film Sheeting 2007;23:63–78.

[52] Borcia C, Borcia G, Dumitrascu N. Plasma induced surface modification in relation to polymer characteristics. J Optoelectron Adv Mater

2008;10:675–9.

[53] Kusano Y, Mortensen H, Stenum B, Goutianos S, Mitra S, Ghanbari-Siahkali A, et al. Atmospheric pressure plasma treatment of glassy carbon for adhesion improvement. Int J Adhes Adhes 2007;27:402–8.

[54] Gunther S, Teuscher N, Heilmann A, Hansel R, Voigt HM, Kiesow A. In-line investigations of atmospheric pressure plasma processes in correlation with surface analysis. J Adhes Sci Technol 2011;25:857–68.

[55] Fricke K, Steffen H, von Woedtke T, Schroder K, Weltmann KD. High rate etching of polymers by means of an atmospheric pressure plasma jet. Plasma Process Polym 2011;8:51–8.

[56] Abenojar J, Colera I, Martinez MA, Velasco F. Study by XPS of an atmospheric plasma-torch treated glass: influence on adhesion. J Adhes Sci Technol 2010;24:1841–54.

[57] Lommatzsch U, Pasedag D, Baalmann A, Ellinghorst G, Wagner HE. Atmospheric pressure plasma jet treatment of polyethylene surfaces for adhesion improvement. Plasma Process Polym 2007;4:S1041–5.

[58] C.R. Brundle, C.A. Evans, S. Wilson, Encyclopedia of materials characterization, 1992

[59] Metal Handbook, Vol.9 Metallography and microstructures, American society of metals, 1985

[60] A. Schütze, J. Y. Jeong, S. E. Babayan, J. Park, G. S. Selwyn, R. F. Hicks, The atmospheric pressure plasma jet : a review and comparison to other plasma sources, IEE transactions on plasma science, vol.26, no.6, December 1998